EMPLOYING ONLINE DATA FOR DYNAMIC EQUIVALENT MODEL PARAMETER IDENTIFICATION OF LARGE SCALE WIND FARM

by

XUEYANG CHENG

Presented to the Faculty of the Graduate School of

The University of Texas at Arlington in Partial Fulfillment

of the Requirements

for the Degree of

DOCTOR OF PHILOSOPHY

THE UNIVERSITY OF TEXAS AT ARLINGTON

May 2015

Acknowledgements

I would like to express deep gratitude to my supervisor professor, Dr. Wei-Jen Lee for his guidance, encouragement, patience, and support throughout the development of this dissertation and my academic program. I would also like to take this opportunity to convey my sincere gratitude to Dr. Lee for extending his support and guidance leading me to the end of my dream of pursuing a doctoral degree. I would be forever indebted to him for his unwavering support and sound advice during my research.

I wish to thank Dr. William E. Dillon, Dr. Rasool Kenarangui, Dr. David A. Wetz and Dr. Ali Davoudi for their instruction, serving on my dissertation committee, valuable suggestions and review.

I also want to express appreciation to all members of Energy Systems Research Center (ESRC), the University of Texas at Arlington, for all their valuable assistances, discussions, and enjoyable association. Apart from that, I would like to thank all colleagues at PwrSolutions for their support and comments of this dissertation.

Finally, I would dedicate my dissertation to my mother and my sister for serving as my continued source of inspiration for the tenure of my doctoral degree. I am very grateful to them for their love, encouragement and endless support.

March 23, 2015

Abstract

EMPLOYING ONLINE DATA FOR DYNAMIC EQUIVALENT MODEL

PARAMETER IDENTIFICATION OF

LARGE SCALE WIND FARM

Xueyang Cheng, PhD

The University of Texas at Arlington, 2015

Supervising Professor: Wei-Jen Lee

As one of the major renewable energy sources, wind power has experienced a fast growth in recent years. The installed capacity of wind farms has increased dramatically. Similar to other generator facilities, their impacts on power system transient stability and power quality should be carefully studied when large scale wind farms are integrated into the power grid. Therefore, it is necessary to establish an accurate dynamic model of large scale wind farm for researches and engineers. A large scale wind farm may have hundreds of WTGs and the structure of WTGs is very complicated and manufacture dependent. If each machine is represented by detailed model, it will aggravate the already existed “dimension disasters” problem and lead to a quite large, high-order and complex system. What’s more, it is very difficult to know each subsystem’s parameters. Though most models information are provided by the manufacturer, many parameters are always tuned on site. Also, it is often difficult for the utilities to know the operating status of the individual turbines within a farm. Therefore, detailed models of all generators in the farm will be difficult and impractical.

Establishing dynamic equivalent model for a wind farm is a viable method for wind farm modeling. Dynamic equivalence model is less detail, yet accurate for dynamic studies, thus can significantly reduce model complexity with the major characteristics retained.

This dissertation proposes a hybrid procedure for identifying the dynamic equivalent model parameters of a large scale wind farm. This proposed procedure is based on the newly published generic WTGs models. The generic models are standard, public and not specific to any vendor, so that it can be parameterized in order to reasonably emulate the dynamic behavior of a wide range of equipment.

The proposed procedure utilizes a new and intelligent method, particle swarm optimization (PSO), to find an approximate solution of the generic WTGs' parameters in the first step. Then the gradient descent search analysis is applied to find more accurate results by using the solution from the first step as initial condition. The proposed PSO-Gradient Search method can provide the right balance between solution accuracy and computational burden. The dissertation also uses system reduction and key parameter identification approach to reduce the computation burden. Phasor measurement units (PMUs) serve as an on-line data collecting source to record the system response.

The proposed procedure is applied on wind farm dynamic equivalence task on both PSS/E SAVNW case and Electric Reliability Council of Texas (ERCOT) system. The encouraging results of these two cases reveal the potential of proposed procedure on identifying the parameters of the dynamic equivalent model of a large scale wind farm.

Table of Contents

List of Illustrations

List of Tables

Chapter 1

INTRODUCTION

1.1 Research Background

Research on wind turbine equivalent model has gained importance because of the rapid increase of wind power industry. Accurate wind turbine generators (WTGs) models is the base of accurate simulation results which are an integral part of power system planning, protection, and operational strategies to ensure reliable power system operation [1]. Inaccurate element models and parameters is an important reason for mismatch between the simulation results and actual system behavior. For example, while the simulation results depicted acceptable post-disturbance performance, the actual system showed poorly damped oscillations of the north-south swing mode associated with the Pacific AC Intertie (PACI) which eventually led to a system blackout during a large disturbance in the Western Electricity Coordinating Council (WECC) system on August, 1996 [2]. Similar experiences were observed during the August 2003 blackout in the United States and Canada [3].

Accurate simulation results can equip system planners and operators with a better knowledge of system reliability, economical operation and safety limits. The accurate models and associated parameters to reflect actual system response have been identified as a key ingredient for transmission planning from a reliability and security standpoint. To ensure simulation accuracy, current North American Electricity Reliability Corporation (NERC) planning standards require that generation equipment shall be tested to verify the data submitted for steady-state and dynamics modeling in planning and operating studies [4]. NERC analysis standards MOD-026-1 and MOD-027-1 also require regular equivalent of models used in planning studies [5, 6]. These standards are so far not mandatory for

wind turbine, but address the necessity on the needs of accurate generating units' model and parameter for the system simulation purpose.

1.2 Dynamic Equivalent Model of Wind Farm

Currently, the size of individual WTGs is usually limited to several megawatts [7]. Therefore, a large wind farm typically consists of hundreds of individual WTGs. Though dynamic behavior of wind farms can be represented by individual detailed models where the dynamics of each individual WTG are fully represented, it will create tremendous computational burden and make the study less efficient. Meanwhile, most dynamic models for WTGs have been developed by manufacturers and consultants as proprietary user-defined models. This type of modeling approach poses a major roadblock for efficiently performing planning studies since it essentially makes the cross platform examination become very difficult or even near impossible [8].

Considering these constrains, detailed modeling of WTGs is not suitable for studying the impact of the entire wind farm on the dynamic behavior of a large scale power system. The complexity of using the detailed modeling of WTGs in a large scale wind farm can be reduced by developing equivalent models. All the WTGs in the wind farm are aggregated into one or several equivalent WTG operating within an equivalent internal electrical network.

The newly developed generic WTGs models makes universal equivalence of WTGs possible. In principle, generic WTG models exhibit the following characteristics:

- Allow for an easy exchange of model data between interested parties.
- Facilitate comparisons of system dynamic performance between different simulation programs.

- Allow for the implementation of WTG models in different simulation programs, and provide a mechanism by which manufacturers can tune the model parameters to best represent their equipment, without revealing proprietary information.

As the result of updated development of prototype generic WTG models, four major WTG topologies have been published [9].

These models have now been implemented and validated in two widely used commercial transient stability simulation programs, PSS/e and PSLF.

1.3 The Proposed Method

This dissertation proposes a procedure to identifying the parameters of dynamic equivalent model of large scale wind farms by using the on-line measured data. The measured data on the wind farm point of interconnection (POI) bus can fully represent the dynamic performance of the wind farm, thus enables dynamic equivalent model parameter identification of wind farms via measured data. Compared to field test, on-line measurement technology such as Phasor Measurement Unit (PMU) or Digital Fault Recorder (DFR) can provide system dynamic behavior information without shutting down generators.

In the proposed procedure, PMU locating at the POI bus, or boundary bus, is chosen as a data collect source due to PMU's wide use in power system monitoring. The necessary PMU measured data are voltage, angle, active power, and reactive power.

Hybrid dynamic simulation is applied to reduce external system by employing input signal on PMU bus. After system reduction, trajectory sensitivity analysis is used to identify key parameters for further efficiency improvement of the proposed algorithm. Since only key parameters have significant impact on the system response, the number of parameters to be optimized can be deducted and the computational burden can be significantly

reduced without scarifying the accuracy of the model's behavior. Finally, an optimization procedure, PSO-Gradient Search method, is proposed to obtain the adequate values of parameter that can be used to predict the response of the wind farm.

Both PSS/E SAVNW system and Electric Reliability Council of Texas (ERCOT) system are presented as case studies to demonstrate the effectiveness of the proposed approach.

1.4 Assumptions and Contributions

1.4.1 Assumptions

The proposed procedure focuses on identifying the parameters of dynamic equivalent models for large scale wind farm using generic WTGs models. The WTGs' generic models itself are assumed to be correct. This assumption is reasonable since the four public generic WTGs models have been approved their effectiveness and are widely adopted in current market. Also, the PMU measurement data on the grid side are assumed to be accurate so that it could fully represent the system behavior on the POI boundary.

1.4.1 Contributions

In this dynamic equivalent model parameter identification procedure, the system reduction using hybrid dynamic simulation and the key parameter identification to reduce computational burden in simulation. The adoption of on-line data recorded by PMU enables the researchers using easy-accessing monitoring data to identify the dynamic equivalent model parameters.

The proposed PSO-Gradient Search method provides the right balance and trade-off between convergence accuracy and computational speed. It is not dependent on the initial guess and exhibits superior performance in terms of simulation time.

The proposed procedure enable researcher to use one or several generic WTGs models to achieve large scale wind farm equivalence rather than to perform detailed modeling of every WTG in the wind farm. It provides an efficient and practical method which meets the needs of large scale wind farm modeling in today's research and engineering applications.

1.5 Synopsis of Chapters

This dissertation is organized as follows:

Chapter 1 introduces the general background of the wind farm dynamic equivalent model development, current research and application situation, illustrates the importance of this research topic and the motivation and objective of this dissertation.

Chapter 2 reviews the wind power generation development, traditional method for wind turbine generator modeling and its limitation. This chapter also reviews the current PMU installation in the ERCOT.

Chapter 3 introduces the generic wind machine model development and its significant effect on wind farm simulation and model equivalence.

Chapter 4 presents the proposed procedure in detail. The theory of hybrid dynamic simulation, trajectory sensitivity, and PSO-Gradient Search are fully discussed.

Chapter 5 uses a test system and SAVNW system in PSS/E to demonstrate the effectiveness of the proposed procedure. Parameter correlation and eigenvalue analyses on the equivalence results were performed to validate the proposed approach.

Chapter 6 illustrates the implementation of the proposed procedure on a large scale wind farm of ERCOT HWLL 2016 system. The wind farm is represented by a three WTGs subsystem with two most widely used generic WTG models.

Chapter 7 presents the conclusions drawn from the research associated with this dissertation and discusses the opportunity for further research.

Chapter 2

LITERATURE REVIEW

2.1 Overview of wind power development

With continuing developments in technology and falling installation costs, wind power has become a fast-growing energy source, providing renewable electricity while reducing air pollution and global-warming carbon emissions.

From 1997 through to 2014, annual installed capacity of wind grew at an average rate of more than 20 percent. Figure 2-1 shows the global annual installed wind capacity during this period. Global wind power installations increased by 35,467 MW in 2013. The U.S. has installed about 1 GW of wind power in 2013, compared to more than 12 GW the year before due to the political uncertainty surrounding the tax laws [10]. After a slowdown in 2013, the wind industry set a new record for annual installations in 2014, 51,477 MW of new wind generating capacity was added. At the end of 2014, total global cumulative installed capacity of wind power has reached 369,553 MW and increased by 16% compared to the previous year. The record-setting figure represents a 44% increase in the annual market, and is a solid sign of the recovery of the industry after a rough patch in the year 2013. Figure 2-2 shows global cumulative installed wind capacity from 1997 to 2014.

According to the Global Wind Energy Council (GWEC), it is expected that the global wind market will grow at an annual cumulative capacity rate of more than 10 percent over the next five years [10].

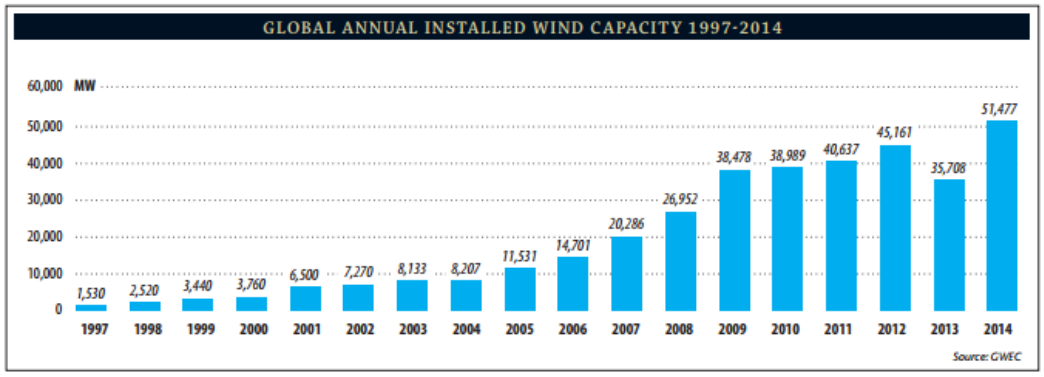

Figure 2-1 Global Annual Installed Wind Capacity 1997-2014 [10]

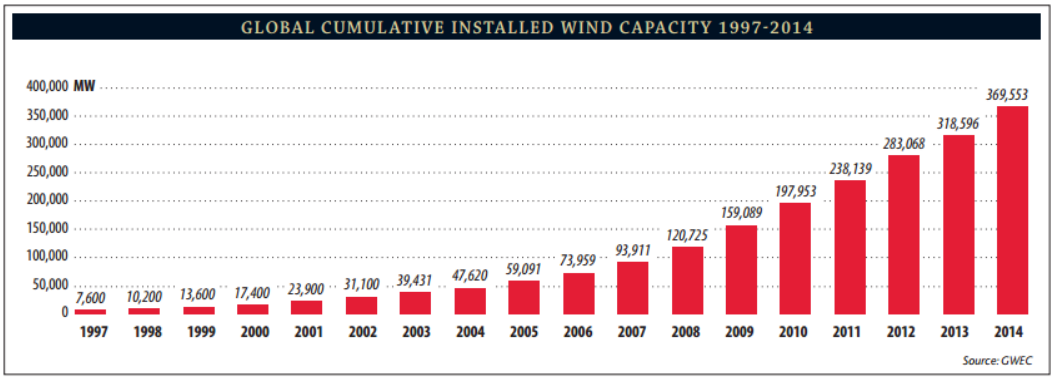

Figure 2-2 Global Cumulative Installed Wind Capacity 1997-2014 [10]

Table 2-1 indicates the wind installation capacity by countries in 2014. China, the U.S. and German were the top three. They all have more than 10% of the market share. The U.S. had a total nameplate wind power capacity of 65,879 MW, ranking 2nd in the global wind market. The U.S. wind power industry has had an average annual growth rate of 25.6% over the last 10 years (beginning of 2005 to end of 2014). For the 12 months through November 2014, the electricity produced from wind power in the United States amounted to 181.15 TWh, or 4.42% of all generated electrical energy.

Table 2-1 Top 10 Cumulative Wind Capacity 2014 [10]

Country	MW	% SHARE
PR China*	114,763	31.0
USA	65,879	17.8
Germany	39,165	10.6
Spain	22,987	6.2
India	22,465	6.1
United Kingdom	12,440	3.4
Canada	9,694	2.6
France	9,285	2.5
Italy	8,663	2.3
Brazil**	5,939	1.6
Rest of the world	58,275	15.8
Total TOP 10	**311,279**	**84.2**
World Total	**369,553**	**100**

Source: GWEC

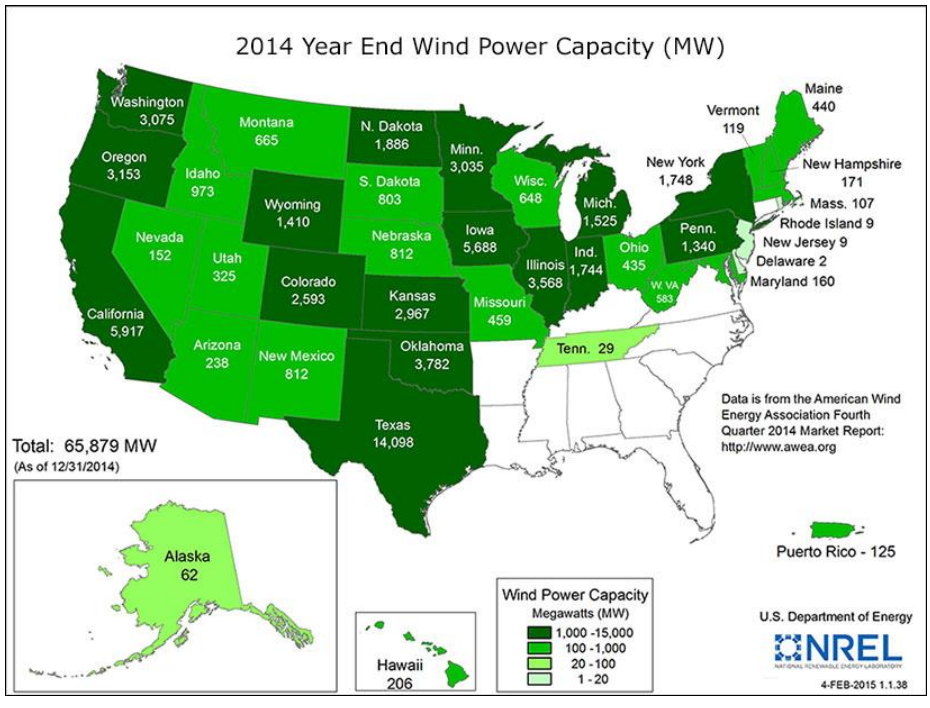

Figure 2-3 Wind Power Capacity in US [11]

As shown in Figure 2-3, Texas is taking the lead of wind power generation within the US. Wind power in Texas consists of more than 40 wind farms with a total installed nameplate capacity of 14,098 MW. Within the ERCOT region, as illustrated in Figure 2-4, wind power capacity will rapidly grow in the next three years and will reach 19,478 MW by 2017 [12]. The biggest surge in new wind power comes in 2015 when more than 3,400 MW is projected to connect to the grid.

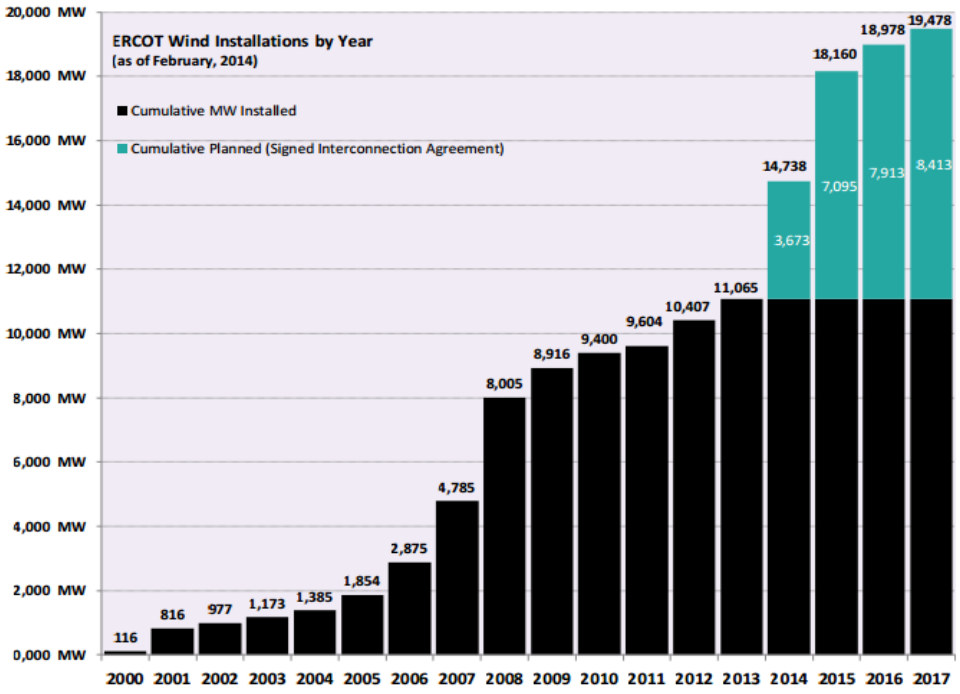

Figure 2-4 Wind Power Capacity in ERCOT [12]

2.2 Dynamic Equivalent Modeling of Wind Farm

With the high penetration of wind power generation in the power system, an accurate model of WTGs is critical for power system simulation. As discussed in Chapter 1.2, detailed modeling of each WTG in a large scale wind farm is a difficult and impractical task, dynamic equivalent models is the right choice for wind farm modeling.

Many studies on equivalent modeling of WTGs have been carried out and some equivalent methods such as coherency-based method, parameter identification and dynamic model equivalent method have been formed gradually [13, 14]. However, the studies on modeling of WTGs are still insufficient.

The dynamic equivalent model research begins from the coherency based equivalent [15, 16]. According to the transient analysis of power system, the generators or motors with similar rotor speed can be clustered into a group [17]. All machines in the same group are integrated into one or several equivalent machines.

Compared with the traditional rotating machines, WTGs has the following features:

1. The input torque of the wind turbine is time varying due to the fluctuations of wind speed. This differs from the constant mechanical torque of synchronous generator and the load torque of induction motor which is a quadratic function of rotor speed. The working point of WTGs may swing in a wide range between zero and maximum output within a very short duration..
2. The control system of WTGs is more complicated. The rotor winding of doubly fed induction generator (DFIG) is fed through two back-to-back PWM converters. Vector-control techniques have been used for decoupled control of active and reactive power drawn from the supply. The blade pitch angle control is used to limit the power and the rotational speed for high winds. The converter power is about 25% of total system power. These features have

greatly increased the economic performance of DFIG. However the reactive power delivered to grid is limited with restrictions imposed by the power electronics in order to avoid excessive temperature rise of converters, rotor slip-rings, and brushes. The maximum reactive power of DFIG depends on stator voltage and stator active power.

3. Different companies such as Vestas, ABB, GE, Siemens, etc. have developed many types of WTGs according to different schemes and situations. These mainly include squirrel-cage induction generator (SCIG), DFIG, permanent magnet synchronous generator (PMSG), etc. A general model doesn't exist due to various principles for various types of WTGs. Each type of WTGs should be considered separately which increases the workload of developing dynamic equivalent model of WTGs.

There are approximately 50 thousand wind turbines making up the U.S. wind turbine fleet of 65,879 MW. The U.S. wind energy supply chain contains 12 utility-scale blade facilities, 14 tower facilities, and 9 turbine nacelle assembly facilities, all spreading across 19 states [18]. Wind turbines produced by various manufactures may have significant difference in their turbines.

Figure 2-5 indicates the wind turbine manufactures market share in the U.S. The top three wind turbine manufacturers, measured by cumulative share of the wind turbine fleet are GE Energy, Vestas, and Siemens. GE Energy captures 40% market share of the cumulative wind turbine fleet, by capacity, followed by Vestas with 19% market share, and Siemens with 14% market share. Six original equipment manufacturers (OEMs) of wind turbines have installed 12 different wind turbine models with a rated capacity of 0.28 MW to 2.85 MW. The average wind turbine installed during 2013 had a rating of 1.87 MW, a hub height 80.3 meters and rotor diameter of 97.0 meters [18].

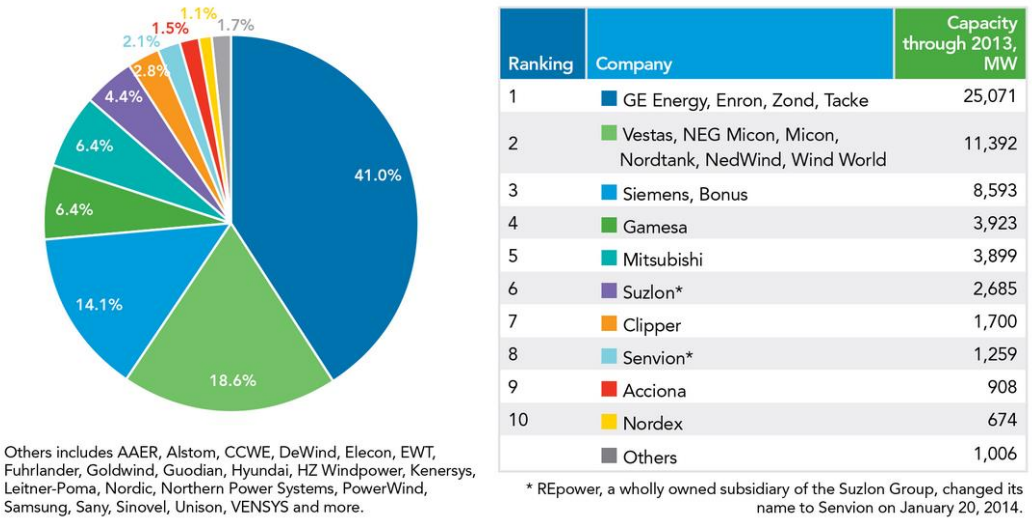

Ranking	Company	Capacity through 2013, MW
1	GE Energy, Enron, Zond, Tacke	25,071
2	Vestas, NEG Micon, Micon, Nordtank, NedWind, Wind World	11,392
3	Siemens, Bonus	8,593
4	Gamesa	3,923
5	Mitsubishi	3,899
6	Suzlon*	2,685
7	Clipper	1,700
8	Senvion*	1,259
9	Acciona	908
10	Nordex	674
	Others	1,006

* REpower, a wholly owned subsidiary of the Suzlon Group, changed its name to Senvion on January 20, 2014.

Figure 2-5 Market Share for Wind Turbine Manufactures of US [18]

The total number of WTGs in a large scale wind farm is so large that it will aggravate the workload if each machine is represented by its detailed model. Also, it is very difficult to know each wind turbine's parameters and working conditions. Besides, the structure of WTGs is more complicated than the traditional generator.

Meanwhile, a large scale wind farms include dozens or even hundreds of WTGs provided by various manufactures. Therefore, the wind farm needs to be aggregated on condition that impacts on power grid at the POI points are wholly retained. This aims to largely reduce the system order and significantly increase the computational speed of simulation.

Table 2-2 shows the summary of large scale wind farms with nameplate capacity higher than 200MW in Texas. Some of the large scale wind farms utilize products from two or even three turbine manufactures, such as Sweetwater Wind Farm.

Table 2-2 Large Scale Wind Farms in Texas [19]

Wind farm	Installed capacity (MW)	Turbine manufacturer	County
Roscoe Wind Farm	781	Mitsubishi	Nolan
Horse Hollow Wind Energy Center	735	GE Energy/ Siemens	Taylor/ Nolan
Capricorn Ridge Wind Farm	662	GE Energy/ Siemens	Sterling/ Coke
Sweetwater Wind Farm	585	GE Energy/ Siemens/ Mitsubishi	Nolan
Buffalo Gap Wind Farm	523	Vestas	Taylor/ Nolan
Panther Creek Wind Farm	458	GE Energy	Howard
Peñascal Wind Farm	404	Mitsubishi	Kenedy
Lone Star Wind Farm	400	Gamesa	Shackelford/ Callahan
Papalote Creek Wind Farm	380	Siemens	San Patricio
Sherbino Wind Farm	300	Vestas	Pecos
Gulf Wind Farm	283	Mitsubishi	Kenedy
King Mountain Wind Farm	278.5	Bonus/ GE Energy	Upton
Pyron Wind Farm	249	GE Energy	Scurry/ Fisher/ Nolan

Based on the above mentioned review, it is necessary to establish an accurate dynamic model for wind farms. However, the burdensome workload for detail modeling, product differences of wind turbines and difficulty of modeling numerous WTGs in large scale wind farms work together to make traditional individual WTG modeling approach computationally prohibitive and impractical.

Dynamic equivalence of WTGs model can significantly avoid the differences of multi-vender WTGs and reduce workload with the major characteristics of WTGs retained. Recently, substantial achievement has been made in generic wind turbine models development. Four basic wind turbine model types have been published by Western Electricity Coordinating Council (WECC), which lays a solid foundation of dynamic equivalence of large scale wind farms [20]. These generic models are standard, publically available, and not specific to any vendor. Any of the WTGs available in the current market can be classified into one of these four generic WTGs types.

In the process of developing dynamic equivalent model of wind farms, the wind farm needs to be aggregated on condition that the performance at the POI points is fully retained. However, more than one equivalent WTGs models corresponding to various manufactures or WTGs with significant difference within a large scale wind farm need to be developed for enhancing the accuracy of dynamics simulation of the wind farm at the POI.

When study the output of a wind farm and its impact on the power system, monitored data on the POI bus gives a comprehensive view of the wind farm's performance. Usually, SCADA system operates with coded signals over communication channels to accomplish the monitoring task on the power grid, but the resolution of the collected data (1 sample for every 2-4 seconds) is not sufficient to describe the dynamic performance of the wind farm.

Intelligent Electronic Devices (IEDs) such as DFRs and PMUs can provide dynamic information with high resolution, which makes dynamic equivalent model development of wind farm become possible.

2.3 PMU Applications in Power System

Synchronized phasor measurements have become a mature technology with several international manufacturers offering commercial phasor measurement units (PMUs) which meet the prevailing industry standard for synchrophasors [21, 22]. PMUs were first introduced in early 1980s, and since then have become a mature technology with many applications which are currently under development around the world [23]. The installation of PMUs on power transmission networks of most major power systems has become an important task. The occurrence of major blackouts in many major power systems around the world has given a new impetus for large-scale implementation of wide-

area measurement systems (WAMS) using PMUs and phasor data concentrators (PDCs) in a hierarchical structure. Data provided by the PMUs are very accurate and enable system analysts to determine the exact sequence of events that helps pinpoint the exact causes to the catastrophic failure of the power system [24].

PMUs monitor the characteristics of power flow on a particular location, for instance, at the point where a generator connects to the bulk power system, or at a substation. The ability to compare time-synchronized data on the same timescale, among widely separated locations, is a relatively new achievement, based on two major improvements:

- Speed. PMUs provide a high scanning resolution — typically 30 times per second — significantly faster than the conventional supervisory control and data acquisition (SCADA) technology, which makes measurement once every few seconds. (For comparison, electricity alternates at a frequency of 60 times per second) The more-frequent measurements from the PMUs can reveal system dynamics that would not be apparent with the older SCADA systems.
- Synchronization. All PMUs across an interconnection are kept in precise time synchronization using GPS, leading to the term "synchrophasor data" (in this context, the term "phasor" comes from the mathematical representation of the measurement). This synchronization provides the capability to easily compare system data among geographical dispersed units, creating wide-area visibility across large power systems, which was not previously possible using older technology.

ERCOT is installing PMUs across its transmission grid, to provide the good observation for entire network. Currently, PMUs are only installed in the networks of participating transmission companies. The geographical locations of the existing PMUs

are shown in Figure 2-6. ERCOT Started with 3 PMUs in 2008, and now over 90 PMUs are installed and connected to ERCOT phasor network.

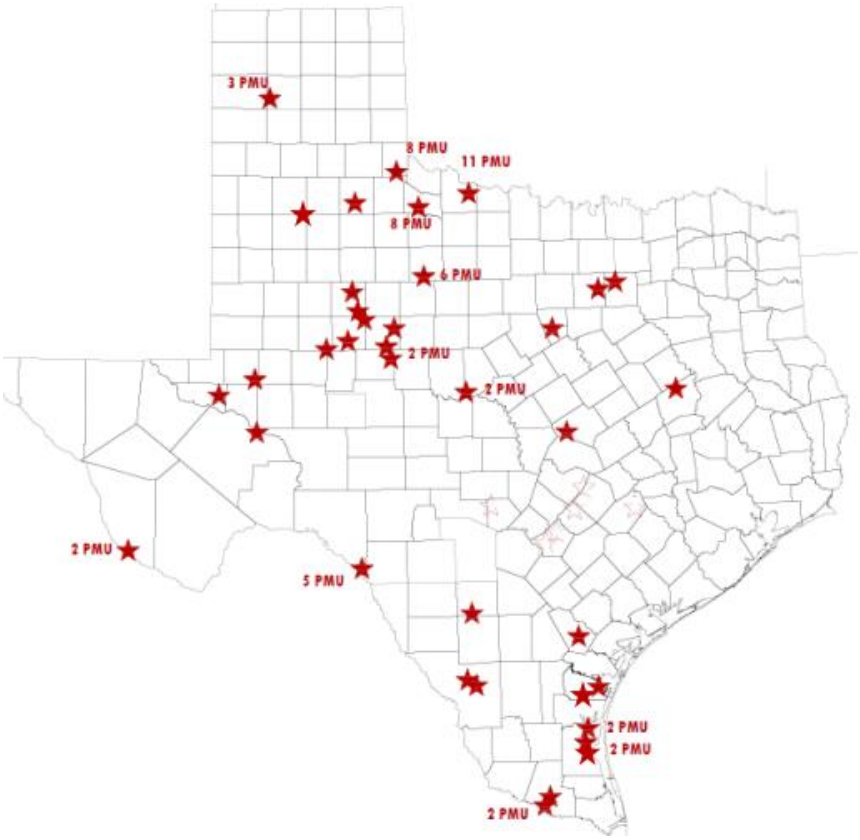

Figure 2-6 PMU Installation in ERCOT

The installed PMUs in current ERCOT grid have already shown that they can be valuable in post-event dynamic analysis, real-time small signal stability monitoring, and dynamic model validation. PMUs installed in the West and North areas allow ERCOT to monitor the stability conditions on West to North interface. Since most of wind generation is installed in West Texas, the data collected from PMUs located close to wind farms can also help ERCOT develop dynamic equivalent models of these wind farms.

Chapter 3

GENERIC WIND MACHINE MODEL DEVELOPMENT

Substantial achievement has been made in generic wind models development in recent years. Presently, there are two industry groups working towards the development of generic and standard models for use in power system stability simulations for wind turbine generators [20]. The first group, which was established in 2005, is the Renewable Energy Modeling Task Force (REMTF) of Western Electricity Coordinating Council (WECC). The second group, which was commissioned in 2009, is the International Electrotechnical Commission (IEC) Technical Committee (TC) 88, Working Group (WG) 27.

3.1 Generic Wind Machine Model

To address the industry need for large scale power system transient stability analysis, the wind Generation Modeling Group (WGMG) of the Western Electricity Coordinating Council (WECC) has embarked on the development of generic positive sequence WTG models [25]. This effort is based on the premise that it technically feasible to develop a generic model for each of the four basic WTG configurations that are currently in use: squirrel-cage induction generator (SCIG), wound-rotor induction generator with adjustable rotor resistance, doubly fed asynchronous generator (DFAG), and a full-power conversion wind turbine generator. Although additional work is required to achieve the stated goals, substantial progress has been made. As an integral part of this WGMG activity, the National Renewable Energy Laboratory (NREL) is also engaged in an extensive model validation project aimed at testing the models against field measurements and refining the WECC generic models as needed.

Despite the large variety of utility-scale WTGs available in the market, each can be classified into one of four basic types, based on the grid interface, as listed below:

- Type 1 – Cage rotor induction generators
- Type 2 – Induction generators with variable rotor resistance
- Type 3 – Doubly-fed asynchronous generators with rotor-side converter
- Type 4 – Full-power converter interface

These four generic models are developed by WECC and are proposed for positive sequence stability analysis of wind turbine generators, for use in power system studies. These models have been released in the latest versions of two commercial software packages Siemens PTI PSS/E and GE PSLF. Figure 3-1 shows the four generic wind turbine generators. In general, the most common technologies in today's market (both in the U.S. and overseas) are the Type 3 and Type 4 units. All the major equipment vendors supply one or both of these technologies. Table 3-1 lists the completed generic models implemented as standard-library models in Siemens PTI PSS™E.

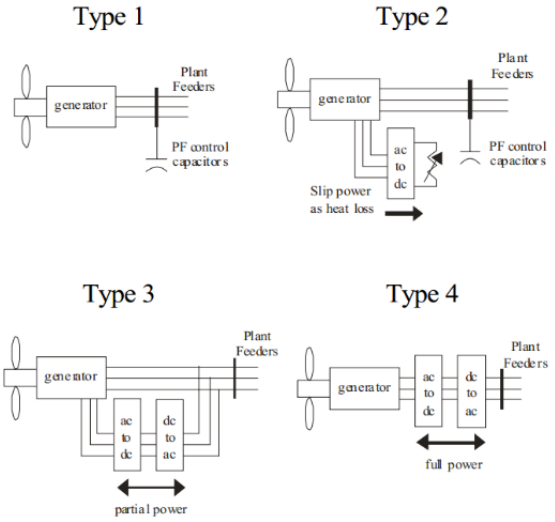

Figure 3-1 Generic Wind Turbine Generators [26]

Table 3-1 Generic WTG Models in PSS/E Library [27]

Generic WTG Modes				
	WT1	**WT2**	**WT3**	**WT4**
Generator Model	WT1G	WT2G	WT3G	WT4G
Electrical Model		WT2E	WT3E	WT4E
Mechanical Model	WT12T	WT12T	WT3T	
Pitch Control Model			WT3P	
Aerodynamic Model	WT12A	WT12A		

3.2 Type 1 and Type 2 Generic Wind Machine Model

Each type of the four WTGs models has fundamentally different characteristics which depend on their structure and the operational manner.

The Type 1 WTG is an induction generator with relatively simple controls. The torque speed characteristic is very steep (about 1% slip at rated torque), which means that these generators operate at nearly constant speed. As with any induction generator, the Type 1 WTGs absorb reactive power. Most commercial Type 1 WTGs use several mechanically switched capacitors (MSCs) to adjust the steady-state power factor at the WTG terminals to unity, over the range of power output. With a slow variation of the wind speed, the individual MSCs switch in and out to follow the varying reactive power demand. A significant reactive power imbalance may occur due to changes in wind speed or grid conditions. Type 1 WTGs pitch the blades to allow the generator to operate at constant mechanical speed even as wind varies.

Type 2 WTGs, similar to Type 1, are induction generators with power factor correction capacitors, and have a similar steady-state behavior. Type 2 WTGs have the capability to rapidly adjust the effective rotor resistance in order to be able to operate at variable slip levels; therefore, the dynamic behavior is very different compared to Type 1 WTGs. The rotor resistance control (fast) and the pitch control (slower) work in harmony to

control speed and reduce mechanical stress. Wind farms with Type 1 and Type 2 WTGs typically have plant-level reactive compensation equipment to meet the steady-state and dynamic reactive power requirements. External reactive power adjustment also helps the plant meet voltage ride-through requirements.

In steady state, Type 1 and Type 2 WTGs are induction generators, and as such, the steady-state power factor is approximately 0.9 leading (absorbing VARs) [26]. Capacitors are added at the generator terminals to correct the power factor. Several capacitor stages are used to maintain steady-state power factor close to unity over the range of output of the WTG. However, these WTGs do not have the ability to control reactive power dynamically. STATCOMS or SVCs are usually needed for Type 1 and Type 2 wind farm to compensate for reactive power losses in the collector system lines and transformers, and to meet reactive control requirements at the point of connection.

In dynamic simulations, Type 1 and Type 2 WTGs are modeled as induction generators with special mechanical and electrical controls [9]. It is important to assign a reasonable power factor to the equivalent Type 1 and Type 2 WTGs in power flow to ensure a clean initialization before performing dynamic simulation. A power factor of approximately 0.9 leading for the generator corrected to unity with a shunt capacitor (assuming nominal voltage) would be a reasonable assumption. This ensures that capacitance added during initialization is kept to a minimum. The WECC power flow guide also discusses this detail [26].

The type 1 wind turbine modeling package includes three main models as follows:

- Generator model WT1G
- Wind turbine model WT12T
- Pseudo turbine-governor model WT12A.

Control block diagram of Type 1 WTG is shown in Figure 3-2.

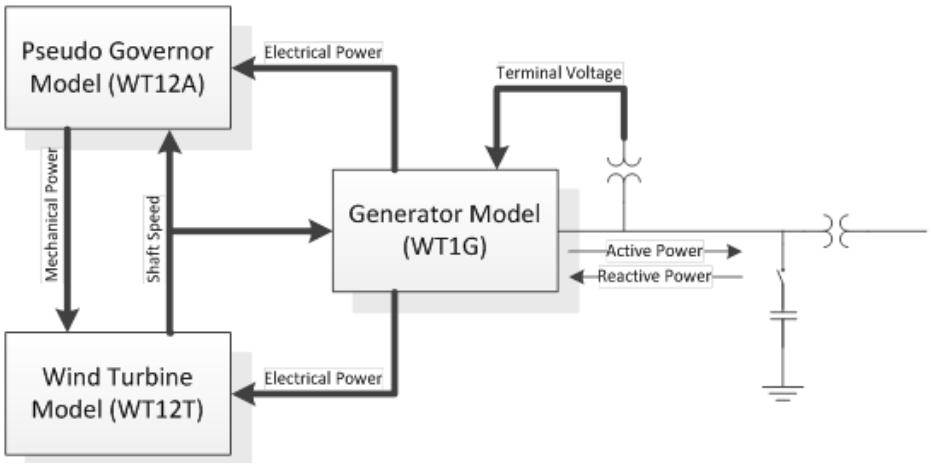

Figure 3-2 Type 1 WTG Model Connectivity Diagram in PSS/E

The type 2 wind turbine package includes four main models as follows:

- Generator model WT2G1
- Rotor resistance control model for the WT2 Generic Wind Model WT2E1
- Two mass turbine model for the WT2 Generic Wind Model WT2T1
- Pseudo-governor model for the WT2 Generic Wind Model WT2A1

Control block diagram of Type 2 WTG is shown in Figure 3-3.

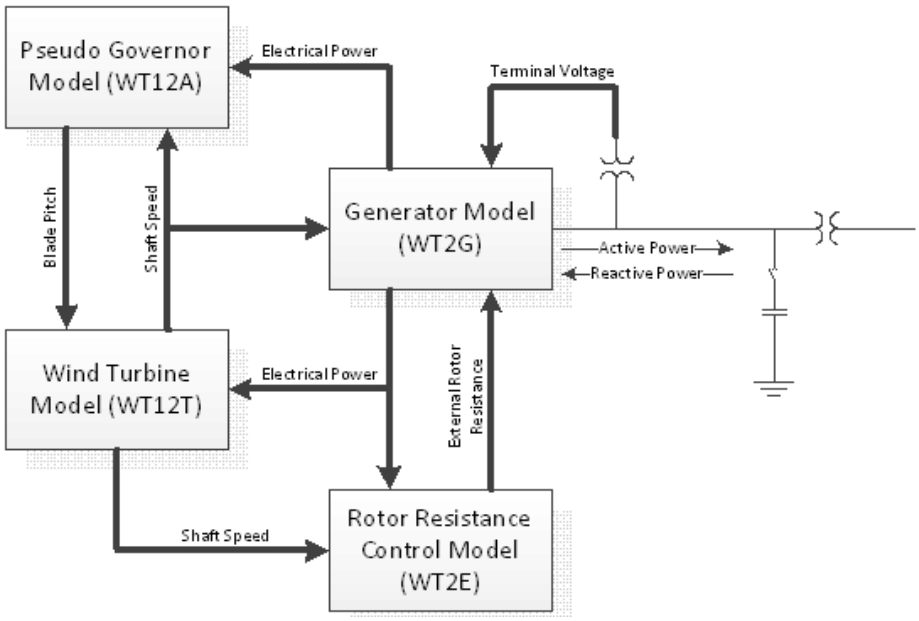

Figure 3-3 Type 2 WTG Model Connectivity Diagram in PSS/E

3.2 Type 3 and Type 4 Generic Wind Machine Model

Type 3 and Type 4 WTGs, in the steady state, have the capability of absorbing or sourcing reactive power. In actual implementation, each Type 3 or Type 4 WTGs follows a power factor reference that can be adjusted dynamically by a plant-level supervisory controller to help achieve a control objective at the point of connection (voltage control or reactive power control) [26]. Faster-acting controls of the WTGs can override the power factor reference to avoid exceeding converter current and terminal voltage limits. Depending on the plant design, additional reactive power support equipment may be installed to meet connection reactive control and voltage ride-through requirements, particularly in weak interconnections.

Obviously, the reactive control ability should be taken into account in the power flow and dynamic representation [9]. For example, if WTGs do not participate in dynamic voltage control (even though they may be technically capable of doing so), then the

dynamic model should reflect a constant power factor. The WECC generic models for the Type 3 and Type 4 WTGs include a volt/var emulator that can be used to simulate the contribution of the WTGs.

Type 3 and Type 4 WTGs do not have power factor correction capacitors installed at the machine terminals, which are different from Type 1 and Type 2 WTGs. The steady-state and dynamic characteristics are controlled by the power converter. Voltage and power factor could be adjusted to a desired value within the rating of the generator and converter. The converters allow the machine to operate over a wider range of speed, and control active and reactive power independently. In this adjustment, the WTGs respond to a reactive power or power factor commands from an external plant-level controller. In Type 3 WTGs, a crow-bar or DC chopper circuit may be used to short the rotor-side converter during a close-in transmission fault, if the rotor-side converter is shorted, the dynamic behavior is similar to an induction generator. On the contrary, the Type 4 WTGs completely isolates the generator from the grid. During a low voltage event, the converter tries to retain full in control of active and reactive currents. Both Type 3 and Type 4 WTGs can be designed to meet low voltage ride-through requirements without external reactive power support. Converters are current-limited devices, and this plays a major role in the dynamic response of Type 3 and Type 4 WTGs to grid disturbances. Type 3 and Type 4 WTGs also have a pitch control to optimize energy capture.

The type 3 wind turbine modeling package includes four main models as follows:

- Generator/Converter Model WT3G
- Electrical control model (converter control) for the Generic Wind Model WT3E
- Mechanical control (wind turbine) for the Generic Wind Model WT3T
- Pitch control model for the Generic Wind Model WT3P

Control block diagram of Type 3 WTG is shown in Figure 3-4.

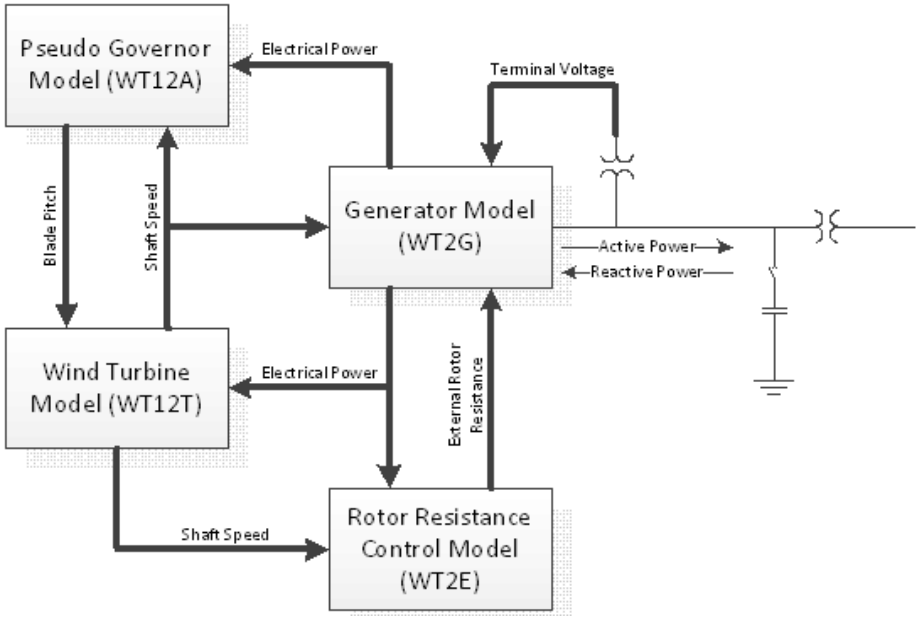

Figure 3-4 Type 3 WTG Model Connectivity Diagram in PSS/E

The type 4 wind turbine package includes two main models as follows:

- Generator/Converter Model WT4G
- Converter Control Model for the Generic Wind Model WT4E

Control block diagram of Type 4 WTG is shown in Figure 3-5.

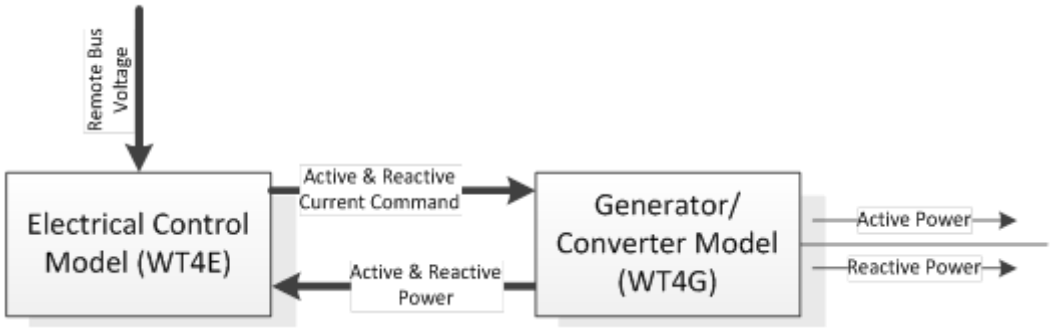

Figure 3-5 Type 4 WTG Model Connectivity Diagram in PSS/E

Chapter 4

PROPOSED PROCEDURE FOR WIND FARM DYNAMIC EQUIVALENT MODEL

4.1 System Reduction

4.1.1 Concept of hybrid Dynamic Simulation

Hybrid simulation is proposed in [28] to incorporate time-series measured records, not only single data points, into simulation programs. Hybrid dynamic simulation has been adopted to establish the dynamic equivalent of the external system. Traditional system reduction method uses equivalent models to replace external system, simulation error is unavoidable. Hybrid dynamic simulation adopts measurement, which accurately records system response, at the point of interconnection (POI) bus, or boundary bus, to represent the external system behavior. An adequate mathematical representation for power systems should capture the nonlinear continuous and discrete dynamics. Such systems, where the system behavior is governed by both discrete and continuous states, are called hybrid systems. Since there is a strong coupling between discrete and continuous behavior of the system, they must be analyzed simultaneously. In power systems, the continuous system behavior at different modes can be described by Differential-Algebraic Equations (DAEs). This method allows for the dynamic simulation of a subsystem with measured signals injected at its boundary without introducing errors from external system.

A hybrid system behavior can be modeled as shown in equations:

$$\dot{x} = f(x, y, z, \lambda) \tag{4.1}$$

$$z = 0 \tag{4.2}$$

$$0 = g^{(0)}(x, y, z) \tag{4.3}$$

$$0 = \begin{cases} g^{(i^-)}(x, y, z, \lambda) & y_{s,i} < 0 \\ g^{(i^+)}(x, y, z, \lambda) & y_{s,i} > 0 \end{cases} \qquad i = 1, ..., s \tag{4.4}$$

$$z^+ = h_j(x^-, y^-, z^-, \lambda) \quad y_{s,i} = 0 \qquad i = 1, ..., r \tag{4.5}$$

(4.1) describes the differential equations, (4.3) and (4.4) are so called switched algebraic equations, and (4.5) are the state reset equations, where

x are continuous dynamic states

y are discrete states

z are algebraic states

λ are parameters of the system

The superscript "-" stands for pre event values and "+" is for post event values. At the beginning, the system behavior is described by the equations given in (4.1) to (4.3). With minor modifications and extensions, the following structure can be used for a modular component model representation.

$$\dot{x}_k = f_k(x_k, y_k, z_k, \lambda_k) \tag{4.6}$$

$$\dot{z}_k = 0 \tag{4.7}$$

$$0 = g^{(0)}(x_k, y_k, z_k) \tag{4.8}$$

$$0 = \begin{cases} g_k^{i^-}(x_k, y_k, z_k, \lambda_k) & y_{k,s}^i < 0 \\ g_k^{i^+}(x_k, y_k, z_k, \lambda_k) & y_{k,s}^i > 0 \end{cases} \qquad i = 1, ..., s \tag{4.9}$$

$$z^+ = h_k^j(x_k^-, y_k^-, z_k^-, \lambda_k) \quad y_{k,r}^j = 0 \qquad i = 1, ..., r \tag{4.10}$$

Where:

- x_k is a vector of continuous dynamic states of the k[th] model

- z_k is a vector of discrete dynamic states of the k[th] model
- y_k is a vector of all algebraic states of the k[th] model
- λ_k is a vector of parameters of the k[th] model
- f_k is a vector of differential equations of the k[th] model
- g_k is a vector of algebraic equations of the k[th] model
- h_k is a vector of state reset equations of the k[th] model

4.1.2 System Reduction Using Hybrid Dynamic Simulation

In power system dynamic simulation study, a huge computational and data collection burden can be avoided by representing the external system with a dynamic equivalent circuit [29]. In system reduction, a part of the system is supposed to be kept and external grid needs to be replaced by equivalent components.

It is the ideal method by employing PMU measurements, which accurately record the system behavior at the boundary between the subsystem and the external system. For a given power system, among active power, reactive power, voltage and angle signal of one point, if two of them are set as input variables, another two could be derived. In hybrid dynamic simulation method, measured data on boundary bus of a subsystem provides an accurate description of system's response, the remaining external system can be reduced by using boundary signal to represent the system behavior [30]. If PMU is installed at the boundary of the subsystem, then the remaining system can be merely represented by the subsystem using the information from the PMU. Therefore, only the models and parameters of the components in the subsystem and the actual measurements on the boundary of the subsystem recorded by PMU are needed for the proposed approach.

The phase shift method, classified as a voltage-injection approach [29], is adopted for the system reduction. In this way, as shown in Figure 4-1, the large scale external grid could be removed and only the target subsystem needs to be kept when injecting the signal to simulate the system response.

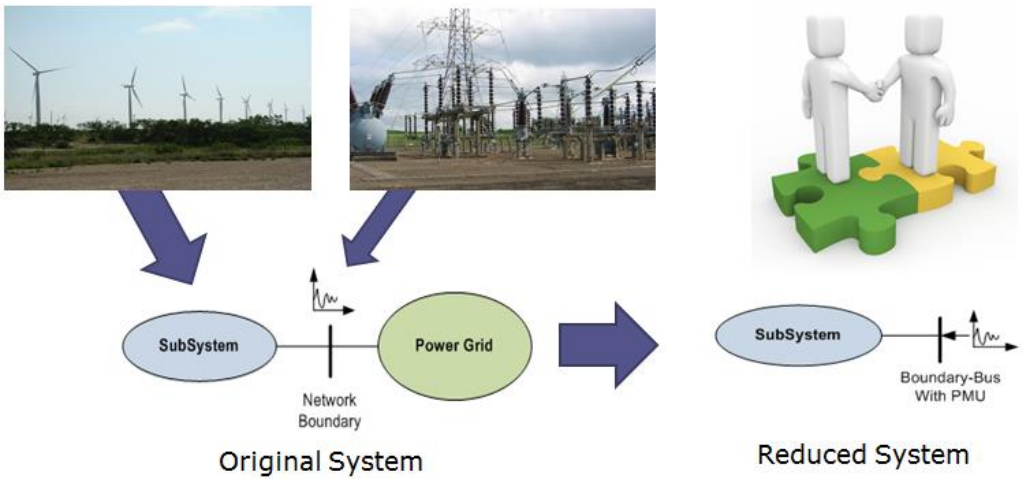

Figure 4-1 System Reduction

In phase shift method, an ideal transformer and a pseudo generator are added at the boundary bus. Figure 4-2 demonstrates this reduction. The inertia of the pseudo generator is assumed to be very large so that the voltage output always keeps at 1 pu, and the reference angle is 0. The transformer's ratio and phase shift are adjusted to match the voltage and angle on the boundary bus in every time step, as shown in (4.11). The active and reactive power output of the boundary bus should match the field measurement data if the parameters of the model inside the subsystem are correct.

$$\begin{cases} n_{ratio} = \dfrac{V_{boundary}}{V_{ref}} \\ \theta_{phase\_shift} = \theta_{boundary} - \theta_{ref} \end{cases} \tag{4.11}$$

Where:

V_{ref} is 1 p.u. and θ_{ref} is 0.

$V_{boundary}$ and $\theta_{boundary}$ are the voltage and angle at the boundary bus, respectively.

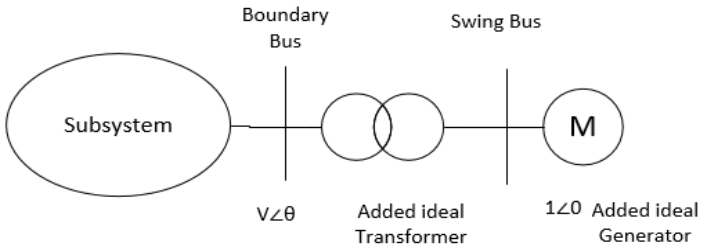

Figure 4-2 Phase Shift Method by Using Hybrid Dynamic Simulation

4.1.3 Application in Test Case

Based on the whole system simulation result, the voltage output of added generator keeps at 1.0 pu and the angle is zero degree. The initial turn ratio (n) of the transformer is set to the initial recorded bus voltage. The initial phase shift (α) of the transformer is set to the initial recorded bus voltage angle.

Figure 4-3 shows the network data of the target subsystem. Boundary bus information is shown in Figure 4-4. In this test case, the target subsystem includes one machine on bus 110003, and the boundary bus is 414000. A transformer connects the wind turbine to the boundary bus.

	Bus Number	Bus Name	Base kV	Area Number/Name	Zone Number/Name	Owner Number/Name
	41400	S_R_B___138A	138.0	4 CNP_TSP	305 CNP_TGN	158 TCNPE
	110003	SRB_SRB_G3	16.5	4 CNP_TSP	906 E_HARRIS	454 ERCOT
*						

Figure 4-3 Subsystem Network Data

In the system reduction, all network information is first deleted except elements in the chosen subsystem. Then ideal buses, branch, transformer and pseudo generator are added at the boundary bus. Bus 1, which the added generator is connected to, should be the swing bus. Ideal transformer is added between bus 1 and bus 2. Bus 2 is connected to boundary bus 41400. The boundary bus information is shown in Figure 4-4. Boundary bus's voltage and angle value are used for the winding 1 ratio and angle of the added transformer. In this test case, the boundary bus (41400)'s voltage is 1.02669 pu (141.683kV), angle is 24.73 degree. After rerunning power flow, the active power and reactive power on the boundary bus is exactly same as the ones in full network power flow case. Figure 4-5 shows the reduced system, the condition on the boundary bus is fully retained through the hybrid dynamic simulation.

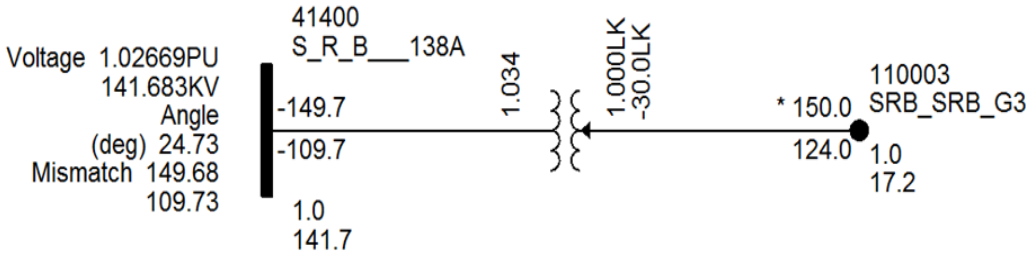

Figure 4-4 Boundary Bus Information

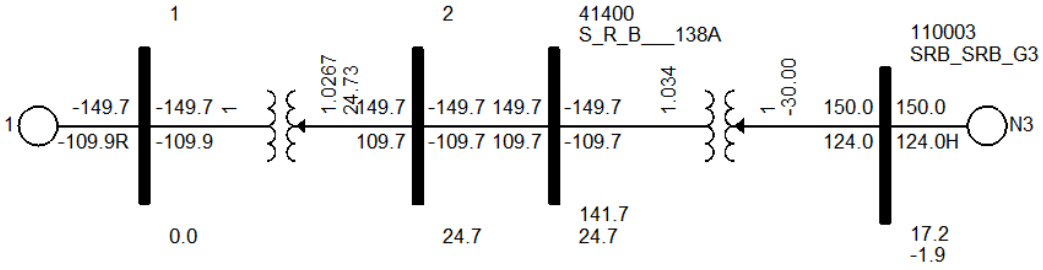

Figure 4-5 Reduced System Demonstration

4.2 Parameter Category by Trajectory Sensitivity Analysis

There are more than ten parameters in most of wind turbine models. The parameters number will be multiplied if trying to use more than one generic equivalent WTGs models to represent a large scale wind farm. These large amounts of model parameters make the equivalence problem more complicated and less efficient. Fortunately, not all parameters are critical enough to be incorporated in the estimation process. These parameters are generally categorized into three sets in terms of the purpose of estimation.

1) The zero parameters. Some parameters are set as zero to represent the absence of the corresponding sub-block in the main block of the model.

2) The parameters that have trivial impact on the result of dynamic events.

3) The parameters that have significant impact on the dynamic results.

Categories 1 and 2 are excluded from the parameter estimation process since they are not critical, not used, or seldom tuned. Only the parameters in category 3 are defined as key parameters in equivalence procedure. Thus, the computational burden of the dynamic equivalent model parameter identification procedure can be tremendously reduced.

Trajectory sensitivities analysis can provide a way to quantify the variation of a trajectory corresponding to small changes in the parameters [31]. The following sections provide detailed discussion on the approaches to solve the problems of key parameters identification via trajectory sensitivities analysis.

The influence of parameter variations on system dynamic behavior can be estimated from these sensitivities. High/Low sensitivities indicate that a parameter has a significant/negligible effect on behavior. These insights are helpful for analyzing the

underlying influences on system dynamics, and for assessing the significance of parameter uncertainty.

Power system dynamic behavior often exhibits the interaction between continuous dynamics and state-driven discrete events. Such behavior can be captured by a differential-algebraic model that incorporates the impulsive action and switching (DAIS model). This model is fully described in [32, 33]. To facilitate a clearer presentation of trajectory sensitivity concepts, this paper will use the simpler model (4.12).

$$\dot{x} = f(x), \qquad x(t_0) = x_0 \tag{4.12}$$

Parameters λ can be incorporated through trivial differential equations

$$\dot{\lambda} = 0, \qquad \lambda(t_0) = \lambda_0 \tag{4.13}$$

It is convenient to describe the response of the model (4.12) in terms of the flow of x, defined as follows

$$x(t) = \phi(x_0, t) \tag{4.14}$$

Where $x(\mathrm{t})$ satisfies (4.12), including the initial conditions

$$\phi(x_0, t) = x_0 \tag{4.15}$$

Trajectory sensitivities provide a way of quantifying the variation of a trajectory flow resulting from small changes to parameters and/or initial conditions. To obtain the sensitivity of the flow ϕ to initial conditions x_0, the Taylor series expansion of (4.16) is formed, and higher order terms can be neglected,

$$\begin{aligned} \Delta x(t) &= \frac{\partial \phi}{\partial x_0} \Delta x_0 + \textit{ higher order terms} \\ &\approx \frac{\partial \phi(t)}{\partial x_0} \Delta x_0 = x_{x_0}(t) \Delta x_0 \end{aligned} \tag{4.16}$$

By incorporating parameters via (4.13), system output under initial conditions x_0 can be the reference for parameter sensitivity evaluation. Equation (4.16) describes the change $\Delta x(\mathrm{t})$ at time t along the trajectory, for a given (small) change in initial conditions Δx_0. The time-varying partial derivatives x_{x_0} are known as trajectory sensitivities. The actual sensitivities x_{x_0} are obtained by differentiating (4.12) with respect to x_0, giving

$$\dot{x}_{x_0} = f_x(\mathrm{t})x_{x_0} \tag{4.17}$$

Where

$f_x \equiv \partial f / \partial x$ is a time-varying Jacobian matrix that is evaluated along the trajectory.

Though the linear time-varying equations (4.17) will have higher dimension for large systems, the computational burden is still very small when an implicit numerical integration technique such as trapezoidal integration is used to generate the trajectory.

In this dynamic equivalent model parameter identification procedure, the key parameters can be identified by adjusting a parameter's value and checking the change of the output. The output element is the active power and reactive power on the boundary bus in this study.

$$\begin{cases} \Delta P(t) = \dfrac{\partial P(t)}{\partial X_i}\Delta X_i = P_{X_i}(t)\Delta X_i \\ \Delta Q(t) = \dfrac{\partial Q(t)}{\partial X_i}\Delta X_i = Q_{X_i}(t)\Delta X_i \end{cases} \tag{4.18}$$

Using equation (4.18), the active power and reactive power changes are estimated when only the value of one parameter in the generic model is adjusted. In this procedure, mean squared error (MSE) of active power and reactive power are adopted as the key parameter estimation measures [34]. The MSE of an estimator measures the average of

the squares of the "errors", that is, the difference between the estimator and what is estimated. MSE is a risk function, corresponding to the expected value of the squared error loss or quadratic loss. MSE has the same units of measurement as the square of the quantity being estimated. The difference occurs because the estimator doesn't account for the information that could produce a more accurate estimation. In this study, the difference occurs between the simulation results and the system response comes from the inaccurate model parameters value.

If $\hat{Y}$ is a vector of n predictions, and $\overline{Y}$ is the vector of true values, then the estimated MSE of the predictor is:

$$MSE(\mathrm{Y}) = \frac{1}{n}\sum_{i=1}^{n}(\hat{\mathrm{Y}}_i - \overline{\mathrm{Y}}_i)^2 \tag{4.19}$$

The total MSE value of active power and reactive power is used to determine the mismatch between simulated results and real system response. If the mismatch is larger than predefined threshold, it indicates that the parameter has an obvious impact on system response, and it should be considered as a key parameter. The key parameter criterion can be set up based on practical needs.

4.3 Particle Swarm Optimization

The goal of dynamic equivalent model parameter identification is to match the simulation results with the real system response. Particle swarm optimization (PSO) is a robust stochastic optimization method based upon the behavior of swarms observed in nature [35]. The method captures the concept of social intelligence and co-operation. In PSO, each particle represents a candidate solution and has two properties: position (x_i) and velocity (v_i). The velocity of a particle directs the flight of the particle. A population of

particles, called a swarm, keeps flying around the search space until the stop criteria is satisfied.

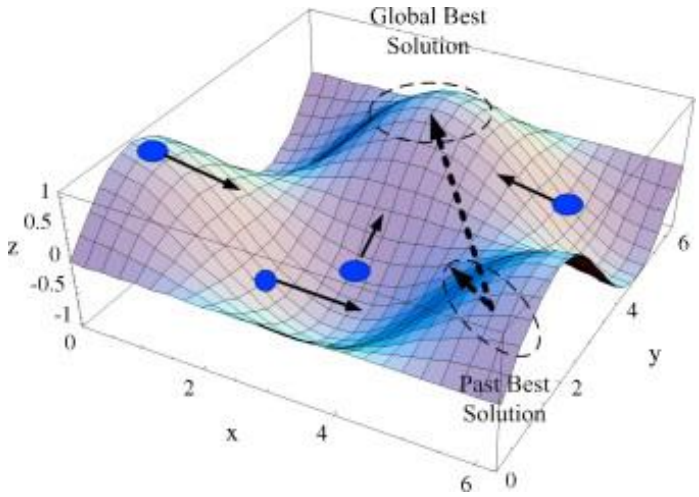

Figure 4-6 Particle Swarm Optimization Method

PSO was developed by a social psychologist- James Kennedy and an engineer- Russell Eberhart in 1995. PSO shares many similarities with some evolutionary computation techniques such as Genetic Algorithms (GA). The system is initialized with a population of random solutions and searches for optima by updating generations. However, unlike GA, PSO has no evolution operators such as crossover and mutation. In PSO, the potential solutions, called particles, fly through the problem space by following the current optimum particles. The PSO method employs particles that exhibit individual and group behavior when looking for a solution within a search space. These particles also have a memory of where they have been. PSO is ideal for complex optimization problems with continuous variables – like finding portfolio or equation weights.

PSO is widely adopted in power system optimization . Power system researchers have applied the PSO technique to solve optimization problems in many areas such as economic dispatch, reactive power and voltage control, state estimation, load flow and

optimal power flow [36]. One of the main advantages of PSO is that it can explore multiple solutions in parallel and utilize a cooperative manner to search for the global best solution. In addition, a good initial guess solution is not required and the algorithm can easily be implemented. However, the drawback of PSO is the slow convergence rate [37].

Essentially, PSO uses the familiar concept of momentum to move particles towards a solution. Figure 4-7 shows the flow chat of PSO Algorithm. Each particle in the swarm is randomly initialized in the problem space. At each step, each particle is updated according to the formulas:

$$v_i^{(k+1)} = w * v_i^k + c_1 * rand_1 * (pbest_i^k - x_i^k) + c_2 rand_2 (gbest^k - x_i^k) \qquad (4.19)$$

$$x_i^{(k+1)} = x_i^k + v_i^{(k+1)} \qquad (4.20)$$

Where:

k is the iteration index.

w is the inertia weight.

x_i^k is the position vector of i^{th} particle at k^{th} iteration.

v_i^k is the velocity vector of i^{th} particle at k^{th} iteration.

c_1 and c_2 are two positive constants. c_1 is the importance of personal best and c_2 is the importance of neighborhood best, respectively.

r_1 and r_2 are two random numbers in range [0, 1].

$pbest_i^k$ is $gbest^k$ the best position of i^{th} particle after k iterations.

$gbest^k$ is the best position of the whole swarm after k iterations.

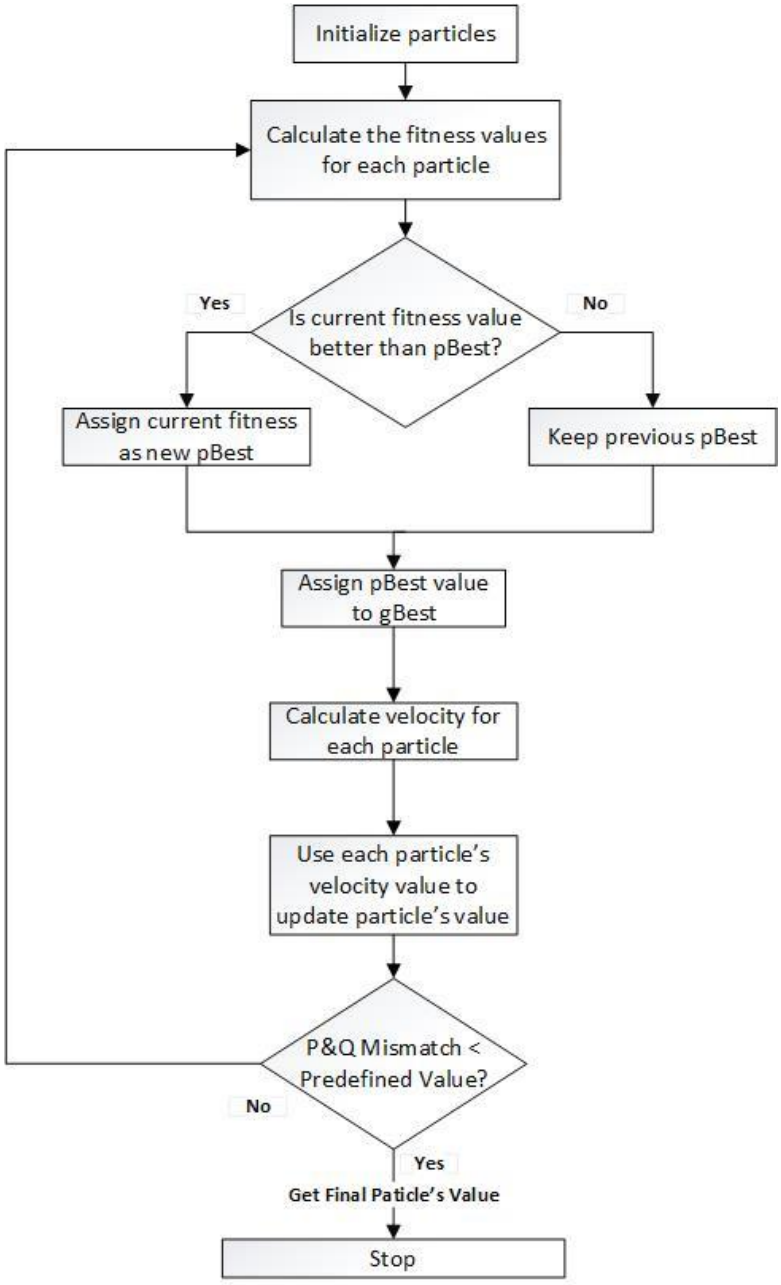

Figure 4-7 Flow Chat of Particle Swarm Optimization Algorithm

4.4 Gradient Descent Search

Gradient descent search is a simple optimization method based on the first derivative of the optimization objective function [38]. It could be combined with PSO method to accelerate the convergence rate to prevent local trap due to its stochastic nature [39, 40].

To find a local minimum of a function using the gradient descent method, one takes steps proportional to the negative of the gradient (or of the approximate gradient) of the function at the current point. If instead, one takes steps proportional to the positive of the gradient, one approaches a local maximum of that function; the procedure is then known as gradient ascent.

Gradient descent method is based on the observation that if the multivariable function $f(\mathrm{x})$ is defined and differentiable in a neighborhood of a point A. Then $f(\mathrm{x})$ decreases fastest if one goes from A in the direction of the negative gradient at A. With this observation, one starts with a guess x_0 for a local minimum of $f(\mathrm{x})$, and considers the sequence $x_0, x_1, x_2, \ldots x_n$ such that

$$x_{i+1} = x_i - \gamma g(x) \tag{4.20}$$

For γ small enough, we have

$$f(x_0) \geq f(x_1) \geq f(x_2) \geq \cdots \tag{4.21}$$

So the sequence X may converges to the desired local minimum.

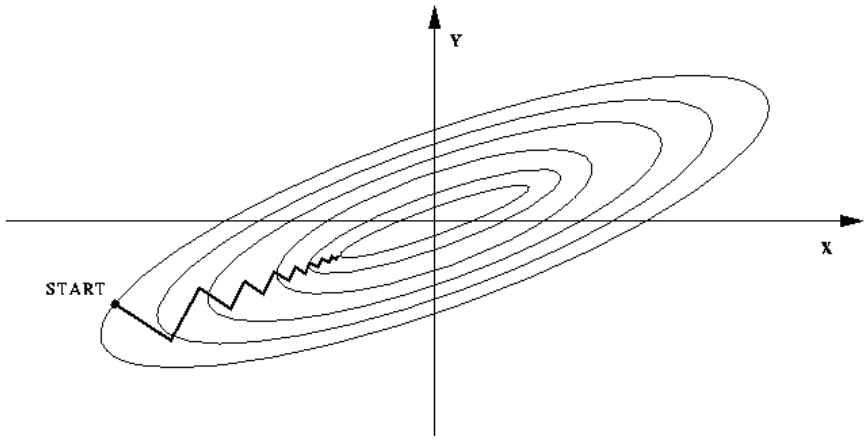

Figure 4-8 Gradient Descent Search Method

4.5 Dynamic Equivalent Model Parameter Identification Procedure

PSO-Gradient Search coordinated algorithm provides the right balance and tradeoff between convergence speed and global solution search ability. This algorithm is not dependent on the initial guess and exhibits the superior performance in terms of simulation time. The coordinated method improves the solution accuracy and computational time of the PSO.

The proposed procedure illustrated in Figure 4-9, identifies parameters of dynamic equivalent models of wind farm by five steps:

a. Extracting event data from PMU. In this step, PMU is assumed to be installed on the boundary bus on subsystem. Active power, reactive power, voltage and angle are recorded.

b. Reducing system by using hybrid dynamic simulation.

c. Identifying key parameters to reduce computational burden.

d. Simulating the same event and comparing the simulated response with the measured result. If obvious mismatch exists, then change of model parameter value is needed.

e. Re-running simulation and parameter optimization until the mismatch converges to a small value.

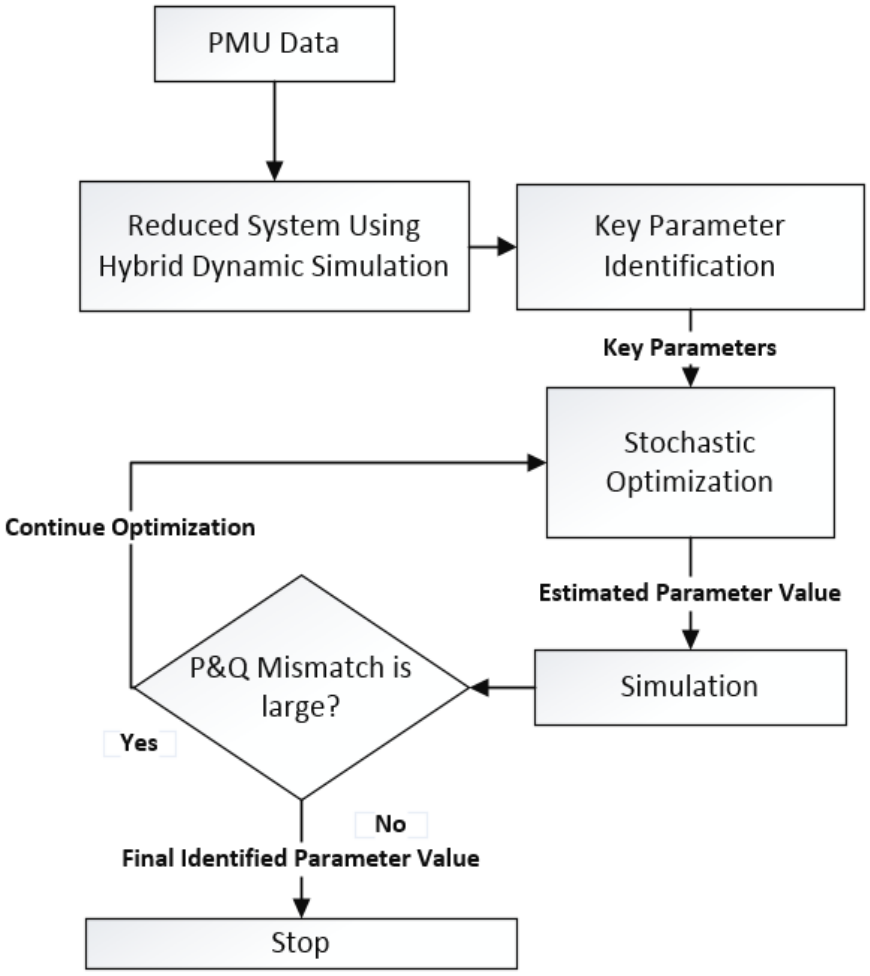

Figure 4-9 Identification of Dynamic Equivalent Model Parameter of Wind Farm

Chapter 5

SAMPLE CASE STUDY

In this chapter, the proposed procedure of dynamic equivalent model parameter identification for wind farms is applied on a PSS/E sample system to demonstrate its feasibility and effectiveness.

5.1 PSS/E Sample System Configuration and Data Set

The PSS/E SAVNW is chosen for this case study. The SAVNW system's complete dynamic data and models are available and public. It consists of 6 generators including gas turbine, nuclear unit and hydro plant. A single wind generator is added in the system to model a wind farm with a total capacity of 28.5MW. The wind farm is connected to bus 151 through a 21.6/500 kV transformer. Bus 151 is assumed to be the boundary bus at which a PMU is located. The wind machine uses generic Type 3 WTG model. Figure 5-1 is the one-line diagram of SAVNW system.

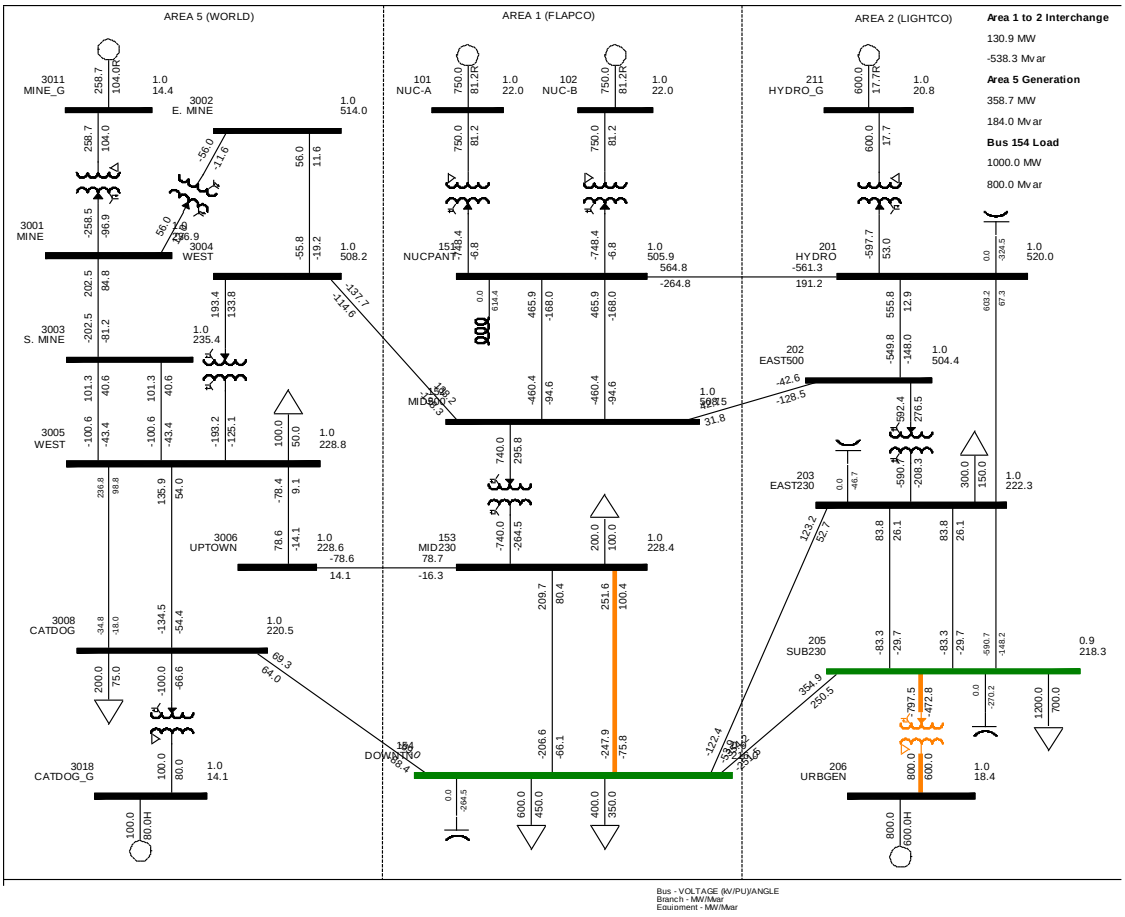

Figure 5-1 One-line Diagram of SAVNW System

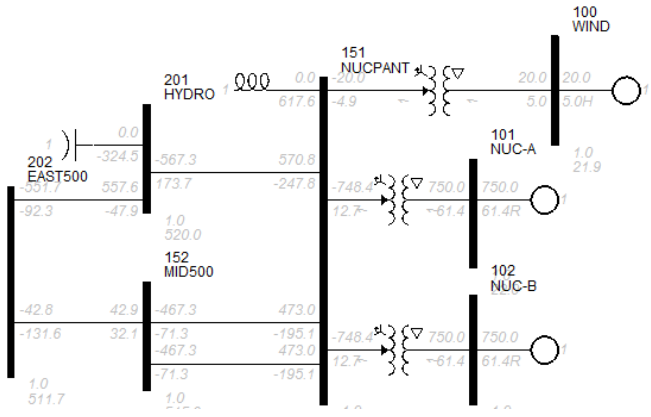

Figure 5-2 One-line Diagram of Subsystem

Figure 5-2 shows the subsystem one-line diagram. A 10 second scenario is described as below:

- Disturbance Location: Bus 202.
- Disturbance Description: A three-phase to ground fault happened at Bus 202 at t=1s, fault was cleared at t=1.1s (6 cycles), then the system ran to t=10s.
- Online data was assumed to be recorded by PMU in Bus 151 including Voltage, Angle, Active Power and Reactive Power.
- Sampling rate is 30/s.

Figure 5-3 to Figure 5-6 illustrate the diagrams of the generator model, electrical model, mechanical model and pitch control model of Type 3 WTG. Table 5-1 to Table 5-4 shows the corresponding model parameters' value.

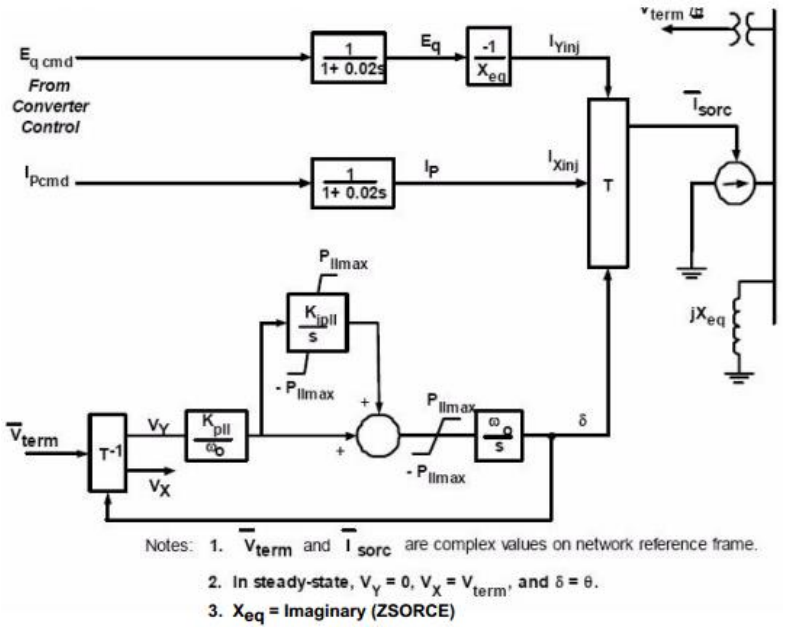

Figure 5-3 Model Diagram of WT3G1

Table 5-1 Model Parameters of WT3G1 (Generator Model)

Con No	Description	Value
1	Xeq	0.8
2	PLL gain	30
3	PLL integrator gain	0
4	PLL maximum limit	0.1
5	Turbine MW rating	0.75

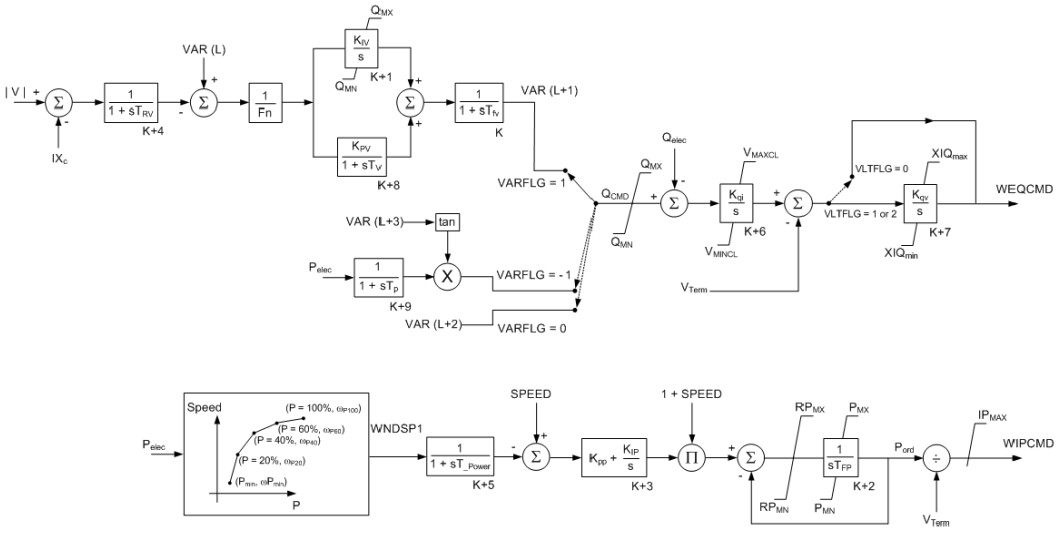

Figure 5-4 Model Diagram of WT3E1

Table 5-2 Model Parameters of WT3E1 (Electrical Model)

Con No	Description	Value
1	Tfv - V-regulator filter	0.15
2	Kpv - V-regulator proportional gain	18
3	Kiv - V-regulator integrator gain	5
4	Xc - line drop compensation reactance	0
5	Tfp - T-regulator filter, seconds (>0)	0.05
6	Kpp - T-regulator proportional gain	3
7	Kip - T-regulator integrator gain	0.6
8	PMX - T-regulator max limit	1.12
9	PMN - T-regulator min limit	0.1
10	QMX - V-regulator max limit	0.296
11	QMN - V-regulator min limit	-0.44
12	IPMAX - Max active current limit	1.1
13	TRV - V-sensor	0.05
14	RPMX - maximum Pordr derivative	0.45
15	RPMN - minimum Pordr derivative	-0.45

Table 5-2 - Continued

16	T_POWER - Power filter time constant, seconds (>0)	5
17	KQi - MVAR/Volt gain	0.05
18	VMINCL	0.9
19	VMAXCL	1.2
20	Kqv - Volt/MVAR gain	40
21	XIQmin - min. limit (see documentation for details)	-0.5
22	XIQmax - max. limit (see documentation for details)	0.4
23	Tv - Lag time constant in WindVar controller	0.05
24	Tp - Pelec filter in fast PF controller	0.05
25	Fn - A portion of on-line wind turbines	1
26	Wpmin, Shaft speed at Pmin, pu	0.69
27	Wp20, Shaft speed at 20% rated power, pu	0.78
28	Wp40, Shaft speed at 40% rated power, pu	0.98
29	Wp60, Shaft speed at 60% rated power, pu	1.12
30	Pwp, Minimum power at Wp100 speed, pu	0.74
31	Wp100, Shaft speed at 100% rated power, pu	1.2

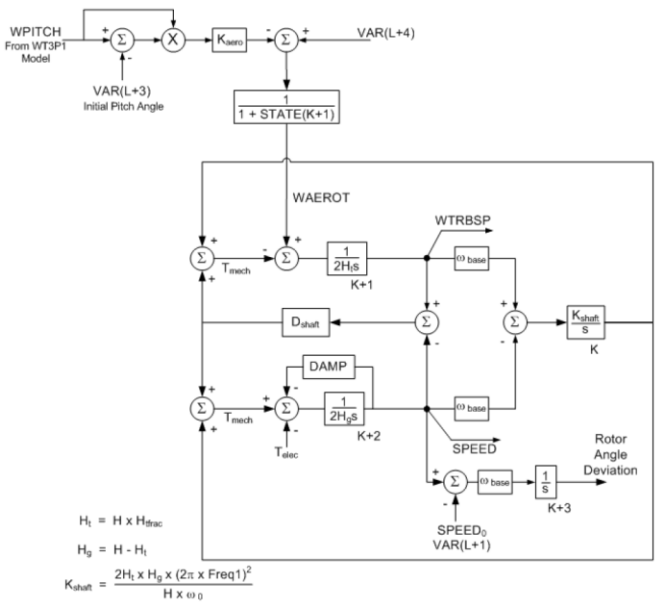

Figure 5-5 Model Diagram of WT3T1

Table 5-3 Model Parameters of WT3T1 (Mechanical Model)

Con No	Description	Value
1	Vw - Initial wind speed, pu of rated wind speed	1.25
2	H - Total inertia constant, MW*sec/MVA	4.95
3	DAMP - Machine damping factor, pu P/pu speed	0
4	Kaero - Aerodynamic gain factor	0.007
5	Theta2 - Blade pitch at twice rated wind speed, deg.	21.98
6	Htfac-Turbine inertia fraction;	0
7	Freq1 - First shaft torsional resonant frequency, Hz	1.8
8	DSHAFT - Shaft Damping factor, pu P/pu speed	1.5

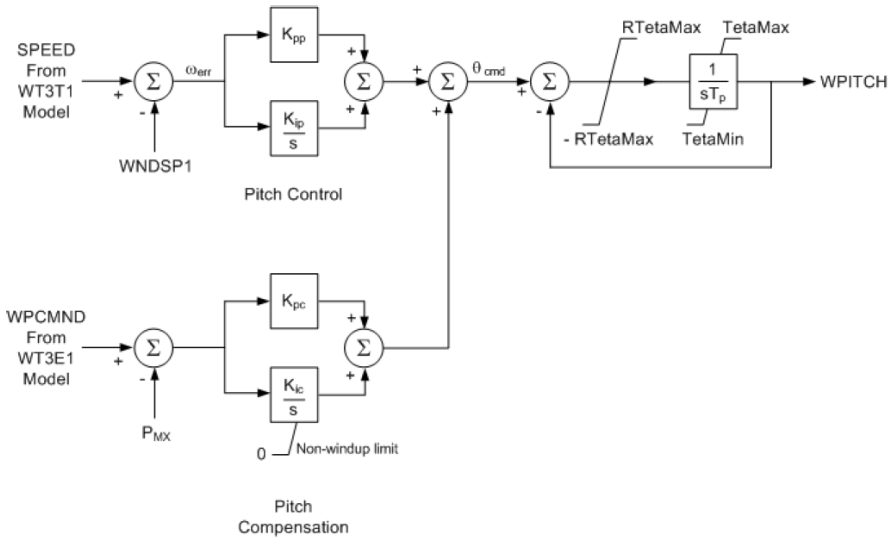

Figure 5-6 Model Diagram of WT3P1

Table 5-4 Model Parameters of WT3P1 (Pitch Control Model)

Con No	Description	Value
1	Tp - Time constant of the output lag (sec)	0.3
2	Kpp - Proportional gain of PI regulator(pu)	150
3	Kip - Integrator gain of PI regulator (pu)	25
4	Kpc - Proportional gain of the compensator(pu)	3
5	Kic - Integrator gain of the compensator (pu)	30
6	TetaMin - Lower pitch angle limit (degrees)	0
7	TetaMax - Upper pitch angle limit (degrees)	27
8	RTetaMax - Upper pitch angle rate limit (deg/sec)	10
9	PMX - Power reference (pu)	1

5.2 System Reduction

During the system reduction process, the elements in the subsystem including generators and transformers connected to the boundary bus 151 are kept while other parts of the SAVNW system are replaced by added generator and transformer. The reduced system is shown in Figure 5-7. The wind unit at bus 100 is the target wind farm. The details of this reduced system are described as follows:

- PMU Boundary Bus: 151
- Target Machine: Machine 1 at Bus 100
- Target Machine Model: Generic Type 3 WTG
- Four models of type 3 WTGs include WT3G1 (Generator), WT3E1 (Electrical), WT3T1 (Mechanical), and WT3P1 (Pitch).

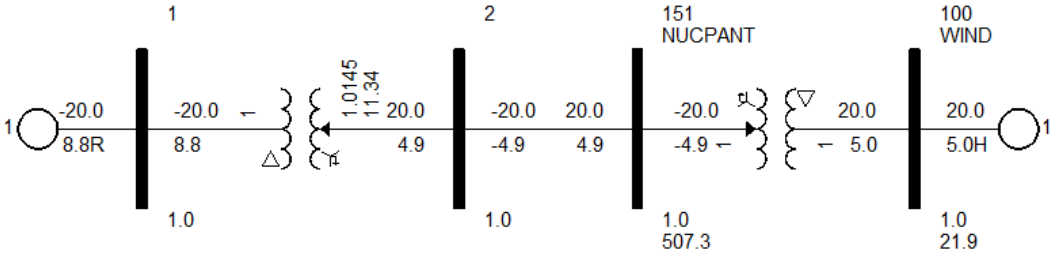

Figure 5-7 Reduced SAVNW System

The system reduction is performed by replacing the outside system with ideal transformer and generator at the boundary bus with the following setting:

- A classical generator model with zero internal reactance, very high inertia constant, and zero damping rations.
- A near zero impedance ideal transformer.
- The turn ratio (n) of the transformer comes from the recorded bus voltage. The phase shift (α) of the transformer comes from the recorded bus voltage angle.

To validate the effectiveness of this system reduction, the comparisons of the active power output and the reactive power output between the whole system simulation and reduced system are shown in in Figure 5-8 and Figure 5-9 respectively. These comparisons indicates that the reduced system is able to retain the dynamic response of the SAVNW system both for the active power output and the reactive power output.

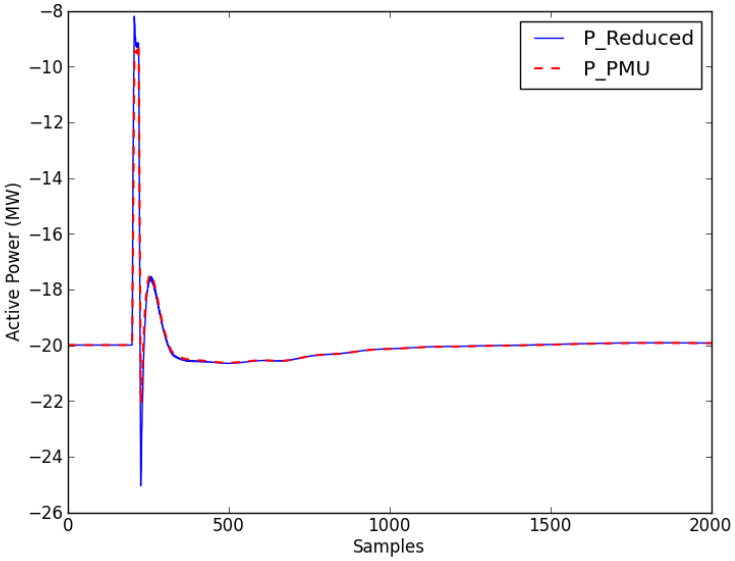

Figure 5-8 Active Power Output Comparison

Whole System and Reduced System Simulation

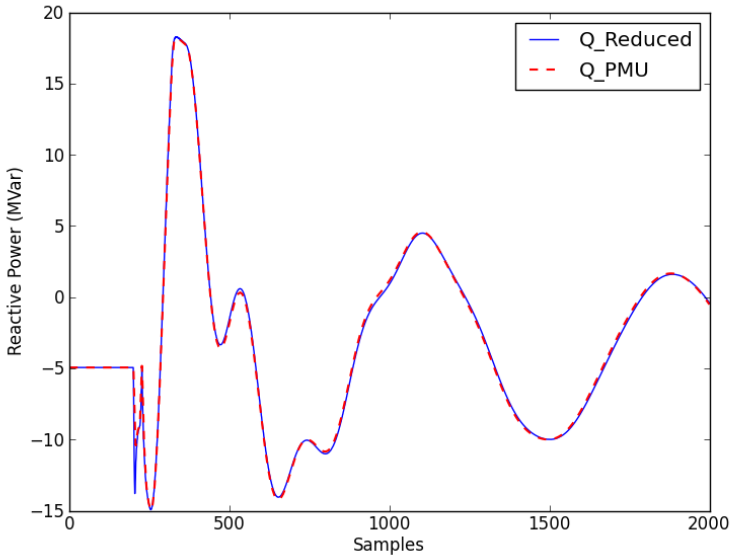

Figure 5-9 Reactive Power Output Comparison

Whole System and Reduced System Simulation

5.3 Key Parameter Identification

According to the previous discussion, key parameter identification aims to obtain a balance between decreasing computational burden and ensuring the validation result accuracy. In this study, if either MSE of active power or reactive power is greater than 0.01, then the parameter is considered as a key parameter. Table 5-5 to Table 5-8 show the MSE analysis result for the four models of the Type 3 WTG.

Table 5-5 MSE Analysis of WT3G1 (Generator Model)

WT3G1 (Generator)					
Con No	Con Value	Con Description	MSE_P	MSE_Q	Key Parameter (Y/N)
1	0.8	Xeq	0.0007	2.7525	Y
2	30	PLL gain	0.0008	0.0027	N
3	0	PLL integrator gain	0	0	N
4	0.1	PLL maximum limit	0	0	N
5	0.75	Turbine MW rating	0.1479	0.0004	Y

Table 5-6 MSE Analysis of WT3E1 (Electrical Model)

WT3E1 (Electrical)					
Con No	Con Value	Con Description	MSE_P	MSE_Q	Key Parameter (Y/N)
1	0.15	Tfv - V-regulator filter	0	0.0011	N
2	18	Kpv - V-regulator proportional gain	0	0.02	Y
3	5	Kiv - V-regulator integrator gain	0	0.0035	N
4	0	Xc - line drop compensation reactance;	0	0	N
5	0.05	Tfp - T-regulator filter, seconds (>0)	0	0.0003	N
6	3	Kpp - T-regulator proportional gain	0.0001	0	N
7	0.6	Kip - T-regulator integrator gain	0	0	N
8	1.12	PMX - T-regulator max limit	0	0	N
9	0.1	PMN - T-regulator min limit	0	0	N
10	0.296	QMX - V-regulator max limit	0	0.0252	Y
11	-0.436	QMN - V-regulator min limit	0	0.0305	Y
12	1.1	IPMAX - Max active current limit	0.005	0.0002	N
13	0.05	TRV - V-sensor	0	0.0009	N
14	0.45	RPMX - maximum Pordr derivative	0	0	N
15	-0.45	RPMN - minimum Pordr derivative	0	0	N
16	5	T_POWER - Power filter time constant	0	0	N
17	0.05	KQi - MVAR/Volt gain	0	0.6881	Y
18	0.9	VMINCL	0	0	N
19	1.2	VMAXCL	0	0	N
20	40	Kqv - Volt/MVAR gain	0	1.2479	Y

Table 5-6 - Continued

21	-0.5	XIQmin - min. limit	0	0.1324	Y
22	0.4	XIQmax - max. limit	0.0001	0.108	Y
23	0.05	Tv - Lag time constant in WindVar controller	0	0.0008	N
24	0.05	Tp - Pelec filter in fast PF controller	0	0	N
25	1	Fn - A portion of on-line wind turbines	0	0.0156	Y
26	0.69	Wpmin, Shaft speed at Pmin, pu	0	0	N
27	0.78	Wp20, Shaft speed at 20% rated power, pu	0.0001	0	N
28	0.98	Wp40, Shaft speed at 40% rated power, pu	0.0003	0	N
29	1.12	Wp60, Shaft speed at 60% rated power, pu	1.0573	0.0007	Y
30	0.74	Pwp, Minimum power at Wp100 speed, pu	0	0.0002	N
31	1.2	Wp100, Shaft speed at 100% rated power, pu	0.0895	0.0001	Y

Table 5-7 MSE Analysis of WT3E1 (Mechanical Model)

WT3T1 (Mechanical)					
Con No	Con Value	Con Description	MSE _P	MSE _Q	Key Parameter (Y/N)
1	1.25	Vw - Initial wind speed, pu of rated wind speed	0	0	N
2	4.95	H - Total inertia constant, MW*sec/MVA	0.0001	0	N
3	0	DAMP - Machine damping factor, pu P/pu speed	0	0	N
4	0.007	Kaero - Aerodynamic gain factor	0	0	N
5	21.98	Theta2 - Blade pitch at twice rated wind speed, deg.	0	0	N
6	0	Htfac-Turbine inertia fraction;	0	0	N
7	1.8	Freq1 - First shaft torsional resonant frequency, Hz	0	0	N
8	1.5	DSHAFT - Shaft Damping factor, pu P/pu speed	0	0	N

Table 5-8 MSE Analysis of WT3P1 (Pitch Control Model)

WT3P1 (Pitch Control Model)					
Con No	Con Value	Con Description	MSE _P	MSE _Q	Key Parameter (Y/N)
1	0.3	Tp - Time constant of the output lag (sec)	0	0	N
2	150	Kpp - Proportional gain of PI regulator(pu)	0	0	N
3	25	Kip - Integrator gain of PI regulator (pu)	0	0	N
4	3	Kpc - Proportional gain of the compensator(pu)	0	0	N
5	30	Kic - Integrator gain of the compensator (pu)	0	0	N
6	0	TetaMin - Lower pitch angle limit (degrees)	0	0	N
7	27	TetaMax - Upper pitch angle limit (degrees)	0	0	N
8	10	RTetaMax - Upper pitch angle rate limit (deg/sec)	0	0	N
9	1	PMX - Power reference (pu)	3E-04	0	N

5.4 Dynamic Equivalent Model Parameter Identification Result

After identifying the key parameters, stochastic approximation method is utilized to detect optimal parameter values to ensure the dynamic response of the model matches the response recorded by the PMU. Particle Swarm Optimization – Gradient Search cooperative method is applied to solve this problem in this study.

Based on the key parameter identification analysis above, only 12 out of 53 parameters are considered as key parameters which only exist in the generator model and electrical model. Hence, the PSO-Gradient Search optimization only need to take these parameters into consideration. 30 PSO iterations and 10 gradient search iterations, which

are enough for the parameters settling down to a stable optimized value, are performed in the optimization process, Figure 5-10 shows that the objective function value, total MSE value of active power and reactive power indicating the mismatch between simulated result and PMU recorded data. The total MSE value decreases fast in the first 7 iterations of PSO optimization. Then the mismatch keeps at the same level. After 30 iterations of PSO optimization, Gradient Search is adopted to accelerate the convergence speed. With 5 iterations of Gradient Search, the objective value gets to 1.2, which is a very small and stable value compared to the start point of this optimization procedure. Then the objective value keeps at the same level.

The optimization results are shown in Table 5-9 and Table 5-10 for WT4G1 and WT3G1 models. The error of several key parameters including Turbine Rating, kpv and Wp100 are comparatively large, most are at a low level.

The comparison results of the active and reactive power output are shown in Figure 5-11 and Figure 5-12 respectively. In this two figures, the red dash lines are the system responses measured by PMU, which are the fitting target of the parameter identification procedure. The black lines are system simulation results using inaccurate WTG model parameter set value. Compared to the real system behavior monitored by the PMU, the simulated responses deviate from the real ones, especially during and after event happened. The blue lines represent the simulation results using identified key parameters values, both the active power and reactive power can fit to the PMU monitored response.

Table 5-9 Optimization Result of WT3G1 (Generator Model)

WT3G1 (Generator Model)					
Con No	Con Value	Con Description	MSE_Total	Calibrated Value	Error (%)
1	0.8	Xeq	2.7532	0.8155	1.937
5	0.75	Turbine MW rating	0.1483	0.6197	-17.37

Table 5-10 Optimization Result of WT3E1 (Electrical Model)

WT3E1 (Electrical Model)					
Con No	Con Value	Con Description	MSE_ Total	Calibrated Value	Error (%)
2	18	Kpv - V-regulator proportional gain	0.02	20.349	13.05
10	0.3	QMX - V-regulator max limit	0.0252	0.258	-14
11	-0.44	QMN - V-regulator min limit	0.0305	-0.421	-4.32
17	0.05	KQi - MVAR/Volt gain	0.6881	0.055	9.8
20	40	Kqv - Volt/MVAR gain	1.2479	41.94	4.85
21	-0.5	XIQmin - min. limit	0.1324	-0.487	-2.66
22	0.4	XIQmax - max. limit	0.108	0.4	0.0475
25	1	Fn - A portion of on-line wind turbines	0.0156	1.152	15.2
29	1.12	Wp60, Shaft speed at 60% rated power, pu	1.058	1.155	3.125
31	1.2	Wp100, Shaft speed at 100% rated power, pu	0.0896	1.06	-11.67

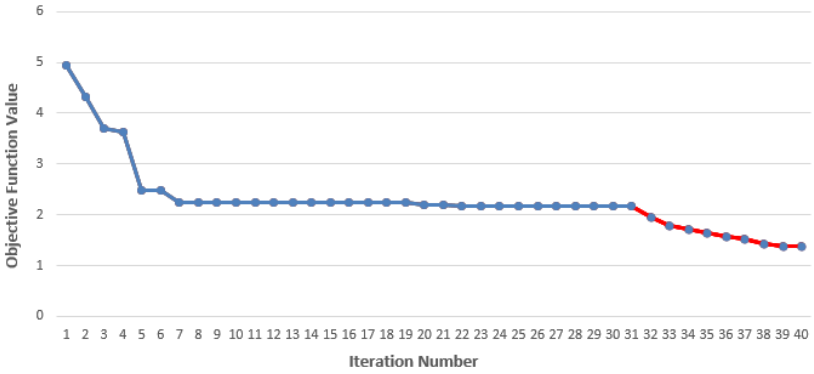

Figure 5-10 Objective Function Value of Optimization

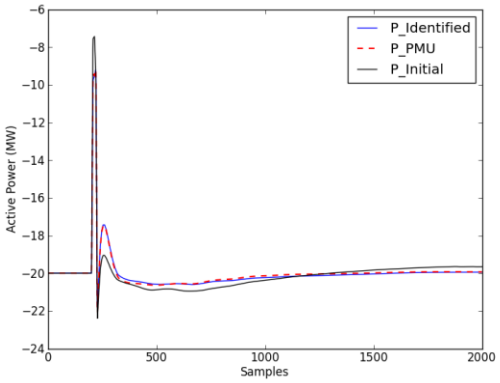

Figure 5-11 Active Power Output Comparison of SAVNW System

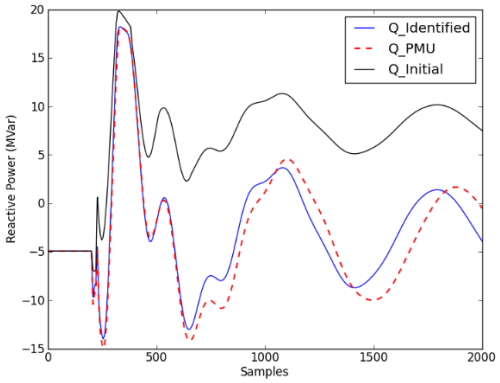

Figure 5-12 Reactive Active Power Output Comparison of SAVNW System

5.5 Parameters Correlation Analysis and Eigenvalue Comparison

Parameter correlation is a common problem for power system state estimation, which results in non-unique parameter values [41]. The interactions between machines and equipment in power plant illustrate their strong dependences. The relationships among them are revealed by the correlation of operational parameters [42]. The system‘s extreme correlation existence leads to the difficultly to uniquely estimate the parameters of wind turbines. Extreme parameter correlation often hampers the estimation of the WTGs model [43].

Usually, the correlation coefficient among parameters can be calculated by operational parameters. Therefore, the uncorrelated and weak correlation parameters can be eliminated from the operational data during the procedure of data analysis and data processing in the operational optimization. The correlation degree of variables is often described by correlation coefficient. For certain sample from the operational parameters in power system, the calculation formula of the correlation coefficients is described as follows.

$$r = \frac{\sum_{i=1}^{n}(x_i - \bar{x})(y_i - \bar{y})}{\sqrt{\sum_{i=1}^{n}(x_i - \bar{x})}\sqrt{\sum_{i=1}^{n}(y_i - \bar{y})}} \tag{5.1}$$

In this study, the optimization aims to obtain one parameter set which can fully simulate the performance of the original system, detecting exact value of every parameter is not necessarily. There exist more than one set of different parameters value to fulfil this goal. Eigenvalue analysis could be used to validate the effectiveness of the optimization result [44]. An eigenvector or characteristic vector of a linear transformation defines a direction that is invariant under the transformation. Let the transformation be defined by the square matrix A, then an invariant direction of A is the non-zero vector v, it has the property that the product Av is a scalar multiple of v. This is written as the equation:

$$Av = \lambda v \tag{5.2}$$

Where λ is known as the eigenvalue associated with the eigenvector v.

Prony's method can be used to estimate eigenvalue of power system response signal [45]. Prony's method was developed by Gaspard Riche de Prony in 1795. It has become a practical use with the support of digital computer. Similar to the Fourier transform, Prony's method extracts valuable information from a uniformly sampled signal and builds a series of damped complex exponentials or sinusoids. This allows for the estimation of frequency, amplitude, phase and damping components of a signal. $f(\mathrm{t})$ is a signal consisting of N evenly spaced samples. Prony's method fits a function:

$$\begin{aligned} \hat{f}(\mathrm{t}) &= \sum_{i=1}^{N} A_i e^{\sigma_i t} \cos(2\pi f_i \,\mathrm{t} + \phi_i) \\ &= \sum_{i=1}^{N} \frac{1}{2} A_i e^{\pm j\sigma_i} e^{\lambda_i t} \end{aligned} \tag{5.3}$$

Where:

$\lambda_i = \sigma_i + j\omega_i$ are the eigenvalues of the system.

σ_i are the damping components.

ϕ_i are the phase components.

f_i are the frequency components.

A_i are the amplitude components of the series.

Using Prony's method to analyze the signal of the system with optimization results and the original system response [46], the eigenvalues is compared in Table 5-11. The eigenvalues of signal (system response) using original data and identified data are similar, which means the optimized result data set could be used to simulate the system behavior.

Table 5-11 Eigenvalue Comparison of SAVNW

Comp No	EIGENVALUE	
	Original Data	Identified Data
1	-0.092+j1.613	-0.090+j1.712
2	0.06	0.064
3	-0.786+j6.778	-0.760+j6.731
4	-1.675+j7.198	-1.826+j7.059
5	-5.036+j9.027	-5.421+j10.262

Chapter 6

APPLICATIONS OF THE PROPOSED PROCEDURE IN ERCOT SYSTEM

6.1 ERCOT System Configuration and Event Scenario

A large scale wind farm modeled by three identical WTGs in the ERCOT system is studied as a test case. ERCOT High Wind Low Load (HWLL) 2016 system network data is used in this study. The wind farm is connected to the ERCOT system through a 34.5 kV line, as shown in Figure 6-1. A PMU has been installed in bus 130021 to record the necessary disturbance signals which is adopted in the dynamic equivalent model parameter identification procedure. Machine at bus 130024 is an equivalent WTG of 107×0.47 MW wind turbines, Machine at bus 130026 is an equivalent WTG of 38×0.75 MW wind turbines, Machine at bus 130028 is an equivalent WTG of 26×2.3 MW wind turbines.

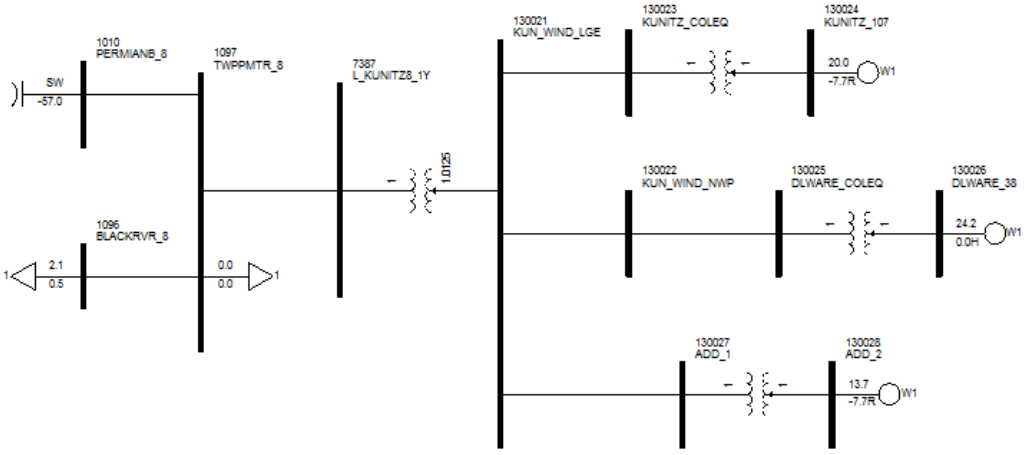

Figure 6-1 One-line Diagram of Studied Subsystem

In Figure 6-1, Generator #1 on bus 130024 is WECC Type 4 WTG. The WT4 modeling package includes two main models: generator/converter model WT4G1 and converter control model WT4E1.

Generator #2 on bus 130026 is WECC Type 3 WTG. The WT3 modeling package includes four main models as follows: generator/converter model WT3G1, electrical control model (converter control) WT3E1; mechanical control (wind turbine) WT3T1, and pitch control model WT3P1.

Generator #3 on bus 130028 is WECC Second Generation Type 4 WTG. The WT4 modeling package includes two main models: generator/converter model WT4G2 and converter control model WT4E2.

The diagrams of these three WTGs' models and the corresponding model parameters' value are listed in Appendix.

In the above-mentioned case study, PMU is assumed to be installed on the boundary bus 130021. Voltage and angle on the boundary bus, active power and reactive power from external system (Bus 96) to boundary bus are recorded. The sampling rate is assumed to be 30 sample/s. In the simulation, a three-phase to ground fault happened at a bus in external system when t=1.0s, the fault lasted 0.05 seconds and then was cleared.

6.2 System Reduction

The system is reduced by replacing the external system with ideal transformer and generator at the boundary bus. An ideal transformer is added at the boundary bus 130021 and an artificial generator is added at bus 1, as shown in Figure 6-2. The generator is a classical generator model with zero internal reactance, very high inertia constant and zero damping rations. The voltage setting for the generator is 1 p.u. The transformer is a near zero impedance ideal transformer. Based on the whole system simulation result, the initial turn ratio (n) of the transformer is set to match the initial recorded bus voltage. The initial phase shift of the transformer is set to match the initial recorded bus angle. During dynamic simulation, the recorded voltage and angle signal are injected as input, while the active

power and reactive power are the response of reduced system. The comparison results of active power and reactive power output between the whole system and reduced system are shown in Figure 6-3 and Figure 6-4, respectively. The comparison indicates that the reduced system is able to retain the dynamic response of the chosen subsystem.

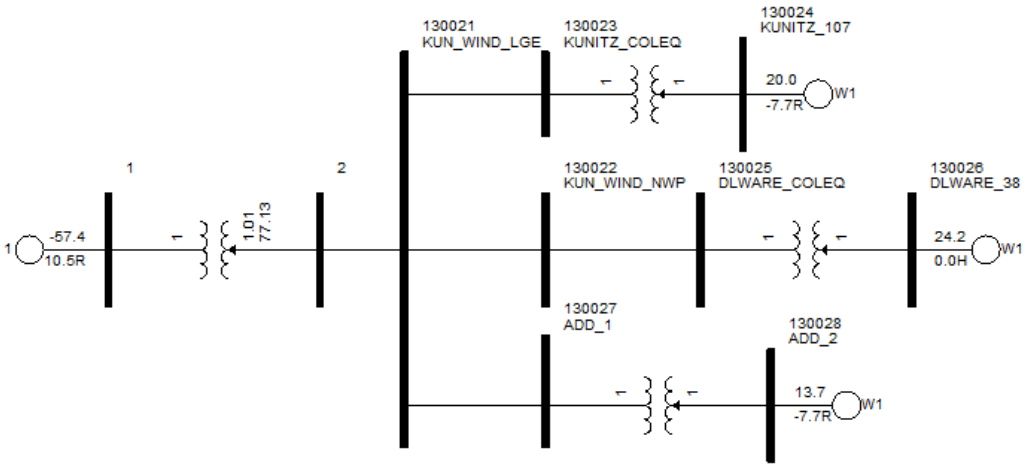

Figure 6-2 One-line Diagram of Reduced System

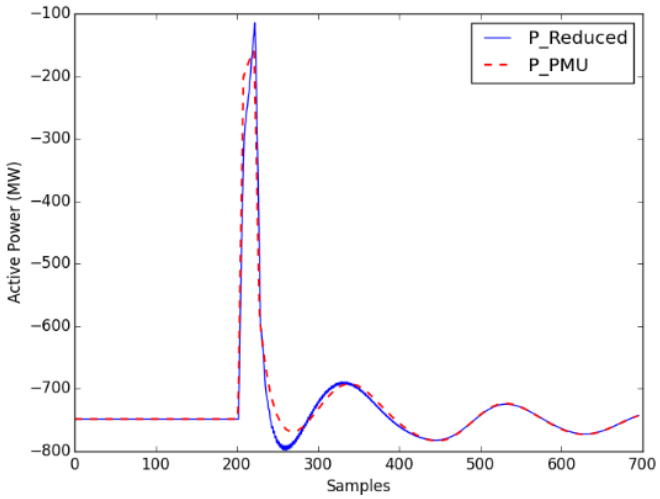

Figure 6-3 Active Power Output Comparison

Whole System and Reduced System Simulation

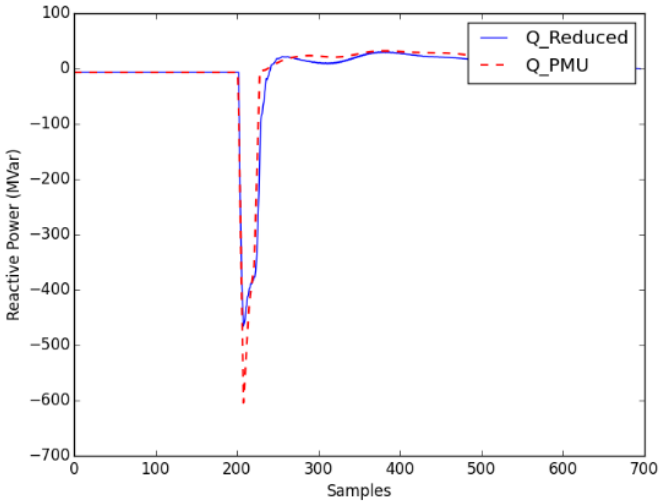

Figure 6-4 Reactive Power Output Comparison

Whole System and Reduced System Simulation

6.3 Key Parameters Identification

Mean Squared Error (MSE) of active power (P) and reactive power (Q) are utilized as an index for the key parameter screening. To evaluate the P and Q output sensitivity to each parameter, every time the value of one target parameter is changed by a certain percentage, which is 5% in this study. this the MSE of P and Q are calculated using:

$$\begin{cases} MSE(P) = \frac{1}{n}\sum_{i=1}^{n}(P_i^{New} - P_i^{Default})^2 \\ MSE(Q) = \frac{1}{n}\sum_{i=1}^{n}(Q_i^{New} - Q_i^{Default})^2 \end{cases} \quad (6.1)$$

P^{New} is the active power output using modified parameter value, $P^{Default}$ is the output using default value. Q^{New} is the reactive power output using modified parameter value and $Q^{Default}$ is the output using default value.

Identifying key parameter needs to achieve a balance between decreasing the computational burden and ensuring the accuracy of optimization result. Decision is made based on MSE value and engineering judgment. In this paper, if MSE of active power or reactive power is greater than 0.001, then the parameter is considered as a key parameter.

Table 6-1 to Table 6-8 show the results of the key parameter screening of all models of the three types WTG.

Table 6-1 MSE Analysis of WT4G1 (Generator Model)

Sensitivity Analysis of Generator Model (WT4G1)				
No	**Con Description**	**MSE_P**	**MSE_Q**	**Key Parameter**
1	TIQCmd, Converter time constant for IQcmd, second	0	0.004	N
2	TIpCmd, Converter time constant for IPcmd, second	0	0	N
3	VLVPL1 - Low Voltage power Logic (LVPL), voltage 1 (pu)	0.0408	0.0005	Y
4	VLVPL2 - LVPL voltage 2 (pu)	0.0461	0.0005	Y
5	GLVPL - LVPL gain	0.0146	0.0001	Y
6	High Voltage reactive Current (HVRC) logic,voltage (pu)	0	0	N
7	CURHVRCR - HVRC logic, current (pu)	0	0	N
8	RIp_LVPL, Rate of active current change	0.0013	0	Y
9	T_LVPL, Voltage sensor for LVPL, second	0.0002	0	N

Table 6-2 MSE Analysis of WT4T1 (Electrical Model)

Sensitivity Analysis of Electrical Model (WT4E1)				
No	**Con Description**	**MSE_P**	**MSE_Q**	**Key Parameter**
1	Tfv - V-regulator filter	0	0.0072	Y
2	Kpv - V-regulator proportional gain	0	0.0007	N
3	Kiv - V-regulator integrator gain	0	0.0002	N
4	Kpp - T-regulator proportional gain	0	0	N
5	Kip - T-regulator integrator gain	0.0002	0	N
6	Kf - Rate feedback gain	0	0	N
7	Tf - Rate feedback time constant	0	0	N
8	QMX - V-regulator max limit	0.0001	0.035	Y
9	QMN - V-regulator min limit	0	0	N
10	IPMAX - Max active current limit	0	0	N
11	TRV - V-sensor	0	0	N
12	dPMX - Max limit in power PI controller (pu)	0	0	N
13	dPMN - Min limit in power PI controller (pu)	0	0	N
14	T_POWER - Power filter time constant	0	0	N
15	KQi - MVAR/Volt gain	0	0.0138	Y
16	VMINCL	0	0	N
17	VMAXCL	0	0	N
18	KVi - Volt/MVAR gain	0	0.0548	Y
19	Tv - Lag time constant in WindVar controller	0	0.0137	Y
20	Tp - Pelec filter in fast PF controller	0	0	N
21	ImaxTD - Converter current limit	0	0	N
22	Iphl - Hard active current limit	0	0	N
23	Iqhl - Hard reactive current limit	0	0	N

Table 6-3 MSE Analysis of WT3G1 (Generator Model)

Sensitivity Analysis of Generator Model (WT3G1)				
No	**Con Description**	**MSE_P**	**MSE_Q**	**Key Parameter**
1	Xeq- equivalent reactance for current injection	0.0027	0	Y
2	PLL gain	0.0017	0	Y
3	PLL integrator gain	0	0	N
4	PLL maximum limit	0	0	N
5	Turbine MW rating	0.0608	0	Y

Table 6-4 MSE Analysis of WT4E1 (Electrical Model)

Sensitivity Analysis of Electrical Model (WT3E1)				
No	**Con Description**	**MSE_P**	**MSE_Q**	**Key Parameter**
1	Tfv - V-regulator filter	0	0.0002	N
2	Kpv - V-regulator proportional gain	0	0.0009	N
3	Kiv - V-regulator integrator gain	0	0.0001	N
4	Xc - line drop compensation reactance; suggested 0.0	0	0	N
5	Tfp - T-regulator filter, seconds (>0)	0	0	N
6	Kpp - T-regulator proportional gain	0.0003	0	N
7	Kip - T-regulator integrator gain	0	0	N
8	PMX - T-regulator max limit	0	0	N
9	PMN - T-regulator min limit	0	0	N
10	QMX - V-regulator max limit	0	0.0035	Y
11	QMN - V-regulator min limit	0	0	N
12	IPMAX - Max active current limit	0.0628	0.0021	Y
13	TRV - V-sensor	0	0.0009	N
14	RPMX - maximum Pordr derivative	0	0	N
15	RPMN - minimum Pordr derivative	0	0	N
16	T_POWER - Power filter time constant, seconds (>0)	0.0001	0	N
17	KQi - MVAR/Volt gain	0	0.0015	Y
18	VMINCL	0	0	N
19	VMAXCL	0	0	N
20	Kqv - Volt/MVAR gain	0	0.0102	Y
21	XIQmin - min. limit (see documentation for details)	0	0	N
22	XIQmax - max. limit (see documentation for details)	0.0004	0.0575	Y
23	Tv - Lag time constant in WindVar controller	0	0.0008	N
24	Tp - Pelec filter in fast PF controller	0	0	N
25	Fn - A portion of on-line wind turbines	0	0.0007	N
26	Wpmin, Shaft speed at Pmin, pu	0	0	N
27	Wp20, Shaft speed at 20% rated power, pu	0	0	N
28	Wp40, Shaft speed at 40% rated power, pu	0.0003	0	N
29	Wp60, Shaft speed at 60% rated power, pu	0.0145	0.0008	Y
30	Pwp, Minimum power at Wp100 speed, pu	0	0	N
31	Wp100, Shaft speed at 100% rated power, pu	0.0311	0.0017	Y

Table 6-5 MSE Analysis of WT4T1 (Mechanical Model)

Sensitivity Analysis of Mechanical Model (WT3T1)				
No	**Con Description**	**MSE_P**	**MSE_Q**	**Key Parameter**
1	Vw - Initial wind speed, pu of rated wind speed	0	0	N
2	H - Total inertia constant, MW*sec/MVA	0.0002	0	N
3	DAMP - Machine damping factor, pu P/pu speed	0	0	N
4	Kaero - Aerodynamic gain factor	0	0	N
5	Theta2 - Blade pitch at twice rated wind speed, deg.	0	0	N
6	Htfac-Turbine inertia fraction; 0 for 1 mass, >0 & <1 for 2 mass model	0	0	N
7	Freq1 - First shaft torsional resonant frequency, Hz	0	0	N
8	DSHAFT - Shaft Damping factor, pu P/pu speed	0	0	N

Table 6-6 MSE Analysis of WT3P1 (Pitch Control Model)

Sensitivity Analysis of Pitch Model (WT3P1)				
No	**Con Description**	**MSE_P**	**MSE_Q**	**Key Parameter**
1	Tp - Time constant of the output lag (sec)	0	0	N
2	Kpp - Proportional gain of PI regulator(pu)	0	0	N
3	Kip - Integrator gain of PI regulator (pu)	0	0	N
4	Kpc - Proportional gain of the compensator(pu)	0	0	N
5	Kic - Integrator gain of the compensator (pu)	0	0	N
6	TetaMin - Lower pitch angle limit (degrees)	0	0	N
7	TetaMax - Upper pitch angle limit (degrees)	0	0	N
8	RTetaMax - Upper pitch angle rate limit (deg/sec)	0	0	N
9	PMX - Power reference (pu)	0	0	N

Table 6-7 MSE Analysis of WT4G2 (Generator Model)

Sensitivity Analysis of Generator Model (WT4G2)				
No	**Con Description**	**MSE_P**	**MSE_Q**	**Key Parameter**
1	TIQCmd, Converter time constant for IQcmd, second	0	0	N
2	TIpCmd, Converter time constant for IPcmd, second	0	0	N
3	VLVPL1 - Low Voltage power Logic (LVPL), voltage 1 (pu)	0	0	N
4	VLVPL2 - LVPL voltage 2 (pu)	0	0	N
5	GLVPL - LVPL gain	0	0	N
6	High Voltage reactive Current (HVRC) logic,voltage (pu)	0	0	N
7	CURHVRCR - HVRC logic, current (pu)	0	0	N
8	RIp_LVPL, Rate of active current change	0	0	N
9	T_LVPL, Voltage sensor for LVPL, second	0	0	N

Table 6-8 MSE Analysis of WT4E1 (Electrical Model)

Sensitivity Analysis of Electrical Model (WT4E2)				
No	**Con Description**	**MSE_P**	**MSE_Q**	**Key Parameter**
1	Tfv - V-regulator filter	0	0	N
2	Kpv - V-regulator proportional gain	0	0.0001	N
3	Kiv - V-regulator integrator gain	0	0	N
4	Kpp - T-regulator proportional gain	0	0	N
5	Kip - T-regulator integrator gain	0	0	N
6	Kf - Rate feedback gain	0	0	N
7	Tf - Rate feedback time constant	0	0	N
8	QMX - V-regulator max limit	0	0.004	Y
9	QMN - V-regulator min limit	0	0	N
10	IPMAX - Max active current limit	0	0	N
11	TRV - V-sensor	0	0	N
12	dPMX - Max limit in power PI controller (pu)	0	0	N
13	dPMN - Min limit in power PI controller (pu)	0	0	N
14	T_POWER - Power filter time constant	0	0	N
15	KQi - MVAR/Volt gain	0	0.0004	N

Table 6-8 - Continued

16	VMINCL	0	0	N
17	VMAXCL	0	0	N
18	KVi - Volt/MVAR gain	0.0014	0.0166	Y
19	Tv - Lag time constant in WindVar controller	0	0.0014	Y
20	Tp - Pelec filter in fast PF controller	0	0	N
21	ImaxTD - Converter current limit	0	0	N
22	Iphl - Hard active current limit	0	0	N
23	Iqhl - Hard reactive current limit	0.0642	0.0003	Y
24	Tiqf - IQmax filter	0	0.0001	N
25	FRT_Thres	0.0035	0.0746	Y
26	FRT_Hys	0	0	N
27	FRT_Droop	0	0	N
28	FRT_Iq_Gain	0.0278	0.0163	Y
29	Max_FRT_Iq	0	0	N
30	IQMax_Fact1	0	0	N
31	IQMax_Fact2	0	0	N
32	DC_Link_Droop	0	0	N
33	VinvMax0	0	0	N
34	Reactor Reactance	0	0	N

6.4 Dynamic Equivalent Model Parameter Identification Result

This three WTGs in this subsystem include 8 models with 128 parameters, within them 25 parameters are considered as key parameters according key parameter identification results. After identifying the key parameters, stochastic approximation method is utilized to detect optimal parameter values to ensure the dynamic response of the models matches PMU recording signal. Particle Swarm Optimization – Gradient Search cooperative method is applied to obtain the optimal parameter value in this case. The optimization results are shown in Table 6-9 to Table 6-13. The error of several key parameters including QMX, kvi and Wp100 are comparatively large, most are at a low level.

Table 6-9 Optimization Result of WT4G1 (Generator Model)

Optimization Results of WT4G1				
No	**Con Value**	**Con Description**	**Identified Value**	**Error (%)**
3	0.4	VLVPL1 - Low Voltage power Logic (LVPL), voltage 1 (pu)	0.402	0.59
4	0.9	VLVPL2 - LVPL voltage 2 (pu)	0.914	1.55
5	1.11	GLVPL - LVPL gain	1.101	-0.82
8	2	RIp_LVPL, Rate of active current change	1.859	-7.03

Table 6-10 Optimization Result of WT4E1 (Electrical Model)

Optimization Results of WT4E1				
No	**Con Value**	**Con Description**	**Identified Value**	**Error (%)**
1	0.15	Tfv - V-regulator filter	0.158	5.53
8	0.47	QMX - V-regulator max limit	0.380	-19.15
15	0.1	KQi - MVAR/Volt gain	0.103	2.75
18	120	KVi - Volt/MVAR gain	144.000	20.00
19	0.05	Tv - Lag time constant in WindVar controller	0.053	5.01

Table 6-11 Optimization Result of WT3G1 (Generator Model)

Optimization Results of WT3G1				
No	**Con Value**	**Con Description**	**Identified Value**	**Error (%)**
1	0.8	Xeq	0.783	-2.09
2	30	PLL gain	29.651	-1.16
5	0.75	Turbine MW rating	0.699	-6.80

Table 6-12 Optimization Result of WT3E1 (Electrical Model)

Optimization Results of WT3E1				
No	**Con Value**	**Con Description**	**Identified Value**	**Error (%)**
10	0.296	QMX - V-regulator max limit	0.289	-2.41
12	1.1	IPMAX - Max active current limit	1.127	2.43
17	0.05	KQi - MVAR/Volt gain	0.050	0.48
20	40	Kqv - Volt/MVAR gain	41.170	2.93
22	0.4	XIQmax - max. limit (see documentation for details)	0.437	9.25
29	1.12	Wp60, Shaft speed at 60% rated power, pu	1.072	-4.25
31	1.2	Wp100, Shaft speed at 100% rated power, pu	0.994	-17.14

Table 6-13 Optimization Result of WT4E2 (Electrical Model)

Optimization Results of WT4E2				
No	**Con Value**	**Con Description**	**Identified Value**	**Error (%)**
8	1	QMX - V-regulator max limit	1.034	3.37
18	55	KVi - Volt/MVAR gain	57.064	3.75
19	0.05	Tv - Lag time constant in WindVar controller	0.049	-1.97
23	1.085	Iqhl - Hard reactive current limit	1.117	2.96
25	0.875	FRT_Thres	0.902	3.06
28	2	FRT_Iq_Gain	2.155	7.76

Figure 6-5 and Figure 6-6 show the active power and reactive power output of the subsystem, respectively. The red dash lines are the PMU recorded data, which is the fitting target of the parameter identification procedure. The output using inaccurate data set of WTG models in simulation are represented by the black lines. It can be observed that the large mismatch of power output between the result of the inaccurate data set and the PMU

recorded. In contrast, when using identified result to perform the simulation, the output of this proposed method represented by blue lines fit to the PMU recorded identically.

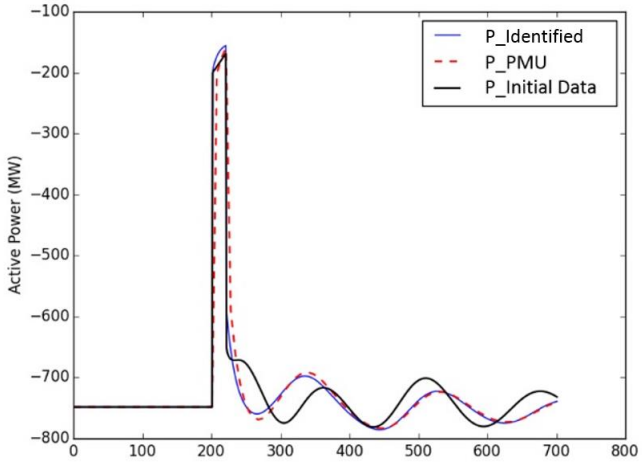

Figure 6-5 Active Power Output Comparison of ERCOT System

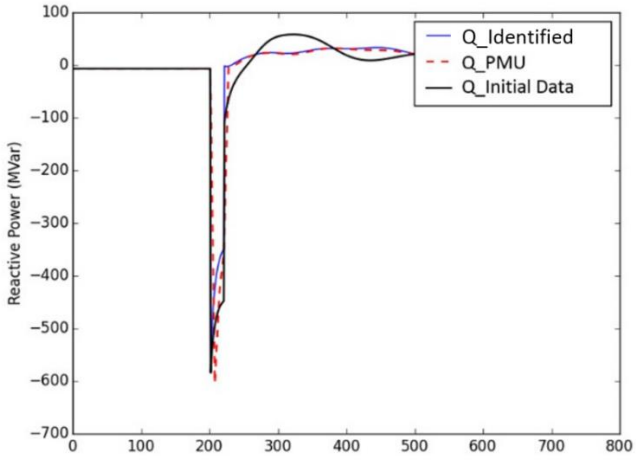

Figure 6-6 Reactive Power Output Comparison of ERCOT System

To exam the feasibility of the optimized result, the eigenvalues of system response using original data and identified data are calculated by Prony's method in Table 6-14. The system eigenvalues with original data and identified data are close enough to ensure the similarity of the system with these two set of model parameters values.

Table 6-14 Eigenvalue Comparison of ERCOT System

Comp No	EIGENVALUE	
	Original Data	Identified Data
1	-0.00967	-0.00971
2	-0.496+j6.247	-0.502+j6.332
3	-0.946	-0.935
4	-1.153+j11.99	-1.12+j12.51
5	-1.297+j12.73	-1.17+j12.62

Chapter 7

CONCLUSIONS AND FUTURE RESEARCH

7.1 Conclusions

Wind power, one of the major renewable energy sources, has experienced a fast growth in recent years. The installed capacity of wind farms has increased significantly. To achieve the full potential of wind power, the industry needs adequate WTGs dynamic models to determine the impact of wind generation integration, and how the system needs to be upgraded. An accurate model of large scale wind farm is in great demand. The total number of wind generators of a large scale wind farm is usually large that the detailed model of the wind farm is computationally prohibitive. Dynamic equivalence technique can be used to significantly reduce the system order as well as retaining the major dynamic characteristics of the WTGs.

Previous studies on equivalent modeling of WTGs usually attempt to build the detailed equivalent model of each WTG, which is an arduous work for the huge amount of WTGs in current market. A large scale wind farm includes hundreds of WTGs, so the detailed modeling of each WTGs in one wind farm for dynamic simulation will be an impractical task.

The generic WTGs model lays a solid foundation of large scale wind farm dynamic equivalent modeling. In the term “generic” is clarified to refer to a model that is standard, public and not specific to any vendor, so that it can be parameterized in order to reasonably emulate the dynamic behavior of a wide range of equipment and at the same time does not directly represent any actual turbine control strategy or divulge proprietary information. The intended usage of these models is primarily for power system stability analysis, with a focus on positive sequence analysis. As the results of the generic model development

activity under the WECC REMTF, four types of generic WTGs models are published for WTGs modeling. These generic WTGs models are the base of the proposed parameter identification of dynamic equivalent models of large scale wind farms in this study.

This dissertation proposes a hybrid two-step method for the dynamic equivalent models parameter identification of large scale wind farms. The proposed method utilizes a new and intelligent method, PSO, to find an approximate solution of the generic WTG data set in the first step. Then, the gradient descent search analysis is applied to improve the accuracy of the result from the approximate solution in the first step. This dissertation also uses a key parameter identification approach to reduce the computational burden. The key parameters of WTGs models are identified through the subsystem boundary bus response tests.

The proposed procedure achieves the target value of the dynamic equivalent model parameter identification on both PSS/E sample case and ERCOT system. Type 3 and Type 4 WTGs, which are mostly adopted in current market, are utilized in two sample studies. The encouraging results demonstrate the effectiveness for applying the proposed method into the power system.

7.2 Potential Future Work

The development of generic WTGs model is still an undergoing effort, future revisions of the models are inevitable. Since these models have been developed in a modular format, such revisions will be more readily implementable. Many of the slight differences between the WECC and IEC versions are presently under discussion by both groups.

This dissertation presents and verifies the proposed large scale wind farm dynamic equivalent model parameter identification procedure. The results show that the proposed

procedure can be a promising solution for solving wind farm modeling problem. There are several future works stemming from this work which could be pursued to improve the accuracy of identification results and to deal with reality application issues as follows:

- Using several results derived from different disturbance events to accurately determine a set of parameters.
- Developing a user-friendly interface to reduce the complexity of program usage.
- Developing an automatic data retrieving process for assessing disturbance records from PMUs, as well as the pre-disturbance power flow case from SCADA.
- Designing a signal noise filter for the disturbance records, if the signals are accompanied by noise.

Appendix A

Model Diagrams and Parameters of ERCOT Subsystem WTGs

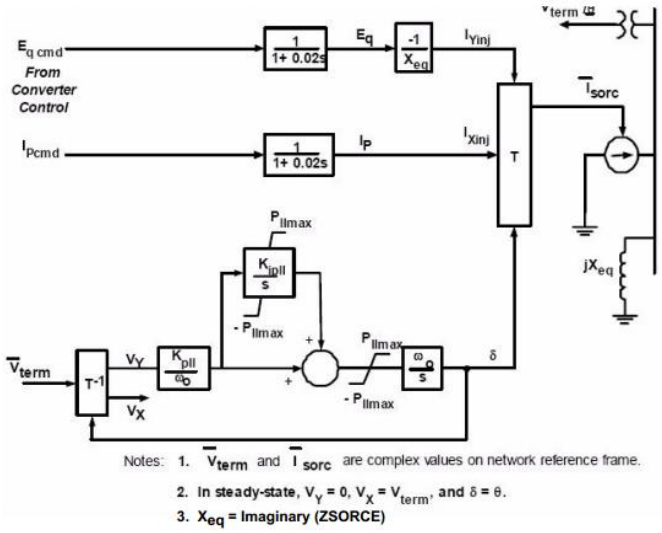

Figure A-1 Model Diagram of WT3G1

Table A-1 Model Parameters of WT3G1 (Generator Model)

Con No	Description	Value
1	Xeq	0.8
2	PLL gain	30
3	PLL integrator gain	0
4	PLL maximum limit	0.1
5	Turbine MW rating	0.75

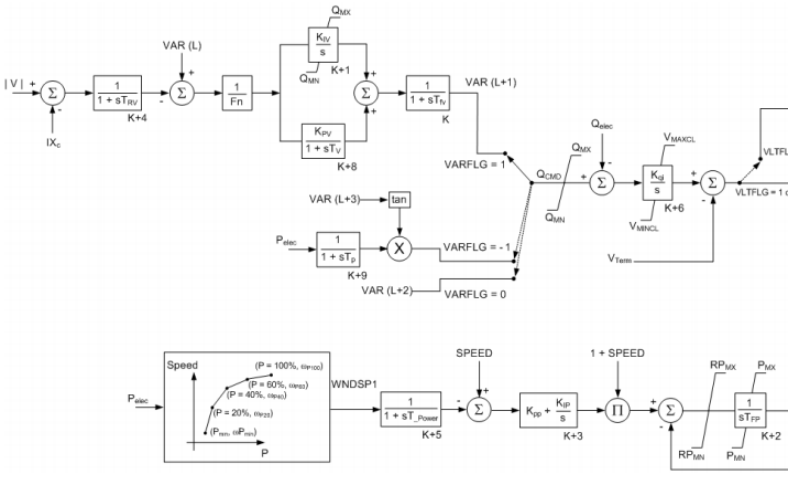

Figure A-2 Model Diagram of WT3E1

Table A-2 Model Parameters of WT3E1 (Electrical Model)

Con No	Description	Value
1	Tfv - V-regulator filter	0.15
2	Kpv - V-regulator proportional gain	18
3	Kiv - V-regulator integrator gain	5
4	Xc - line drop compensation reactance	0
5	Tfp - T-regulator filter, seconds (>0)	0.05
6	Kpp - T-regulator proportional gain	3
7	Kip - T-regulator integrator gain	0.6
8	PMX - T-regulator max limit	1.12
9	PMN - T-regulator min limit	0.1
10	QMX - V-regulator max limit	0.296
11	QMN - V-regulator min limit	-0.436
12	IPMAX - Max active current limit	1.1
13	TRV - V-sensor	0.05
14	RPMX - maximum Pordr derivative	0.45
15	RPMN - minimum Pordr derivative	-0.45
16	T_POWER - Power filter time constant, seconds (>0)	5
17	KQi - MVAR/Volt gain	0.05
18	VMINCL	0.9
19	VMAXCL	1.2
20	Kqv - Volt/MVAR gain	40

Table A-2 - Continued

21	XIQmin - min. limit (see documentation for details)	-0.5
22	XIQmax - max. limit (see documentation for details)	0.4
23	Tv - Lag time constant in WindVar controller	0.05
24	Tp - Pelec filter in fast PF controller	0.05
25	Fn - A portion of on-line wind turbines	1
26	Wpmin, Shaft speed at Pmin, pu	0.69
27	Wp20, Shaft speed at 20% rated power, pu	0.78
28	Wp40, Shaft speed at 40% rated power, pu	0.98
29	Wp60, Shaft speed at 60% rated power, pu	1.12
30	Pwp, Minimum power at Wp100 speed, pu	0.74
31	Wp100, Shaft speed at 100% rated power, pu	1.2

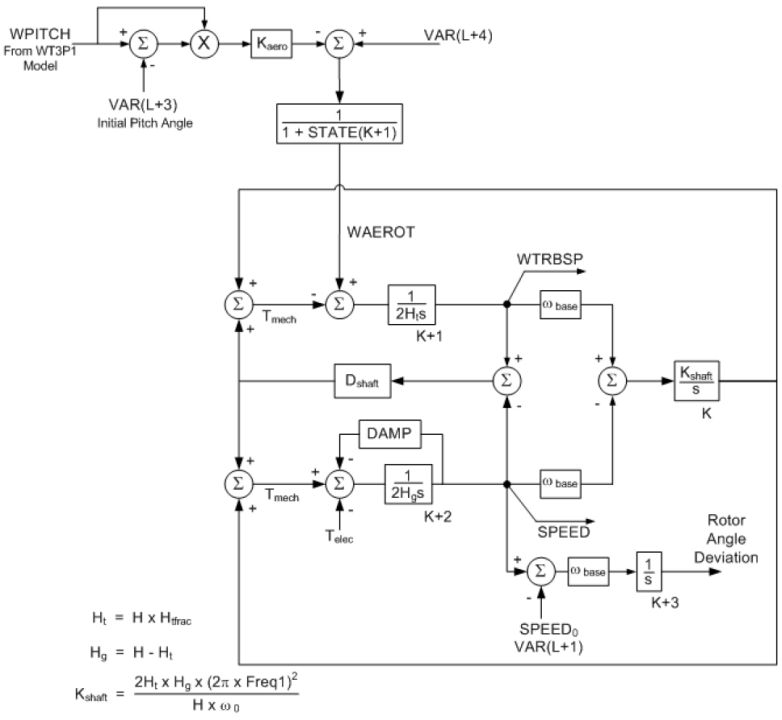

Figure A-3 Model Diagram of WT3T1

Table A-3 Model Parameters of WT3T1 (Mechanical Model)

Con No	Description	Value
1	Vw - Initial wind speed, pu of rated wind speed	1.25
2	H - Total inertia constant, MW*sec/MVA	4.95
3	DAMP - Machine damping factor, pu P/pu speed	0
4	Kaero - Aerodynamic gain factor	0.007
5	Theta2 - Blade pitch at twice rated wind speed, deg.	21.98
6	Htfac-Turbine inertia fraction;	0
7	Freq1 - First shaft torsional resonant frequency, Hz	1.8
8	DSHAFT - Shaft Damping factor, pu P/pu speed	1.5

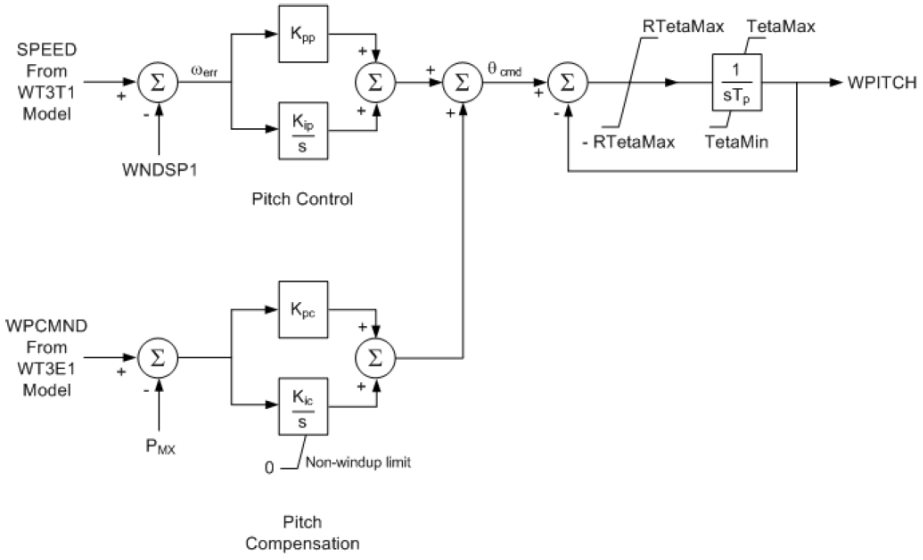

Figure A-4 Model Diagram of WT3P1

Table A-4 Model Parameters of WT3P1 (Pitch Control Model)

Con No	Description	Value
1	Tp - Time constant of the output lag (sec)	0.3
2	Kpp - Proportional gain of PI regulator(pu)	150
3	Kip - Integrator gain of PI regulator (pu)	25
4	Kpc - Proportional gain of the compensator(pu)	3
5	Kic - Integrator gain of the compensator (pu)	30
6	TetaMin - Lower pitch angle limit (degrees)	0
7	TetaMax - Upper pitch angle limit (degrees)	27
8	RTetaMax - Upper pitch angle rate limit (deg/sec)	10
9	PMX - Power reference (pu)	1

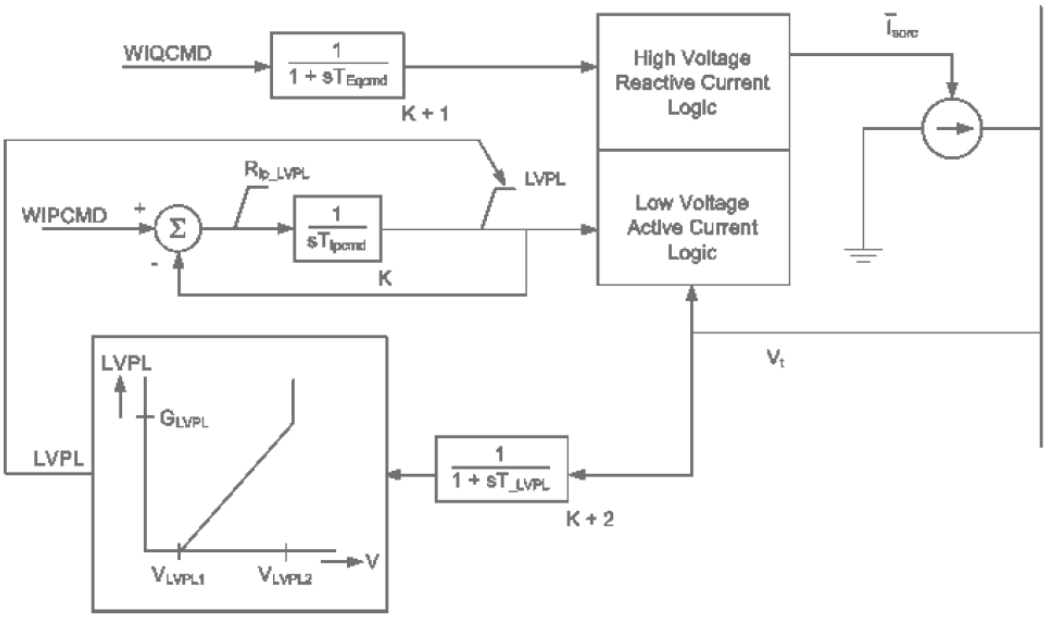

Figure A-5 Model Diagram of WT4G1 and WT4G2

Table A-5 Model Parameters of WT4G1 (Generator Model)

Con No	Description	Value
1	TIQCmd, Converter time constant for IQcmd, second	0.02
2	TIpCmd, Converter time constant for IPcmd, second	0.02
3	VLVPL1 - Low Voltage power Logic (LVPL), voltage 1 (pu)	0.4
4	VLVPL2 - LVPL voltage 2 (pu)	0.9
5	GLVPL - LVPL gain	1.11
6	High Voltage reactive Current (HVRC) logic,voltage (pu)	1.2
7	CURHVRCR - HVRC logic, current (pu)	2
8	RIp_LVPL, Rate of active current change	2
9	T_LVPL, Voltage sensor for LVPL, second	0.02

Table A-6 Model Parameters of WT4G2 (Generator Model)

Con No	Description	Value
1	TIQCmd, Converter time constant for IQcmd, second	0.001
2	TIpCmd, Converter time constant for IPcmd, second	0.002
3	VLVPL1 - Low Voltage power Logic (LVPL), voltage 1 (pu)	0.4
4	VLVPL2 - LVPL voltage 2 (pu)	-0.1
5	GLVPL - LVPL gain	1.11
6	High Voltage reactive Current (HVRC) logic,voltage (pu)	1.25
7	CURHVRCR - HVRC logic, current (pu)	2
8	RIp_LVPL, Rate of active current change	2
9	T_LVPL, Voltage sensor for LVPL, second	0.02

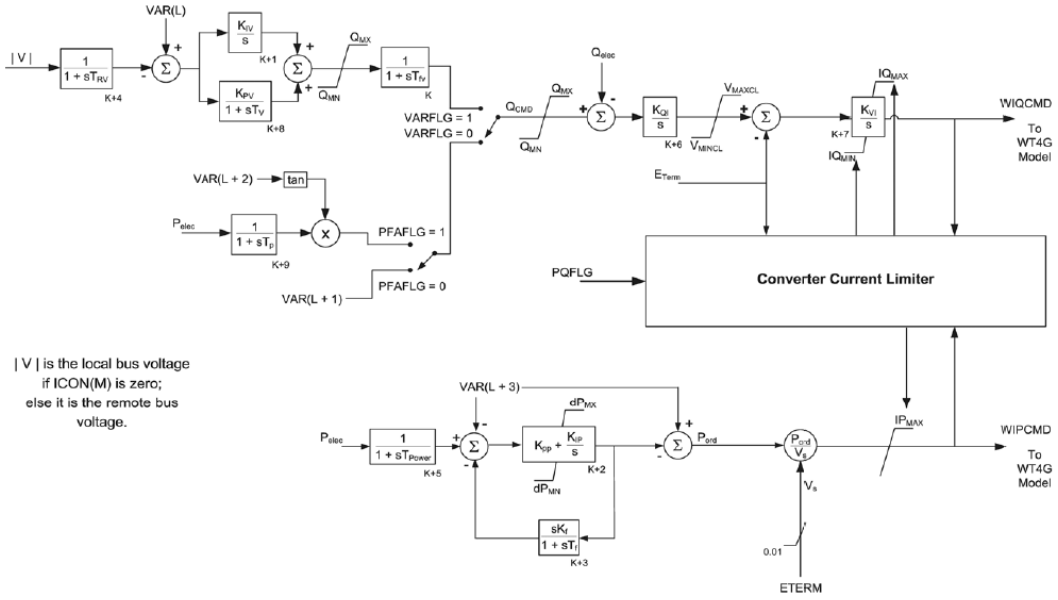

Figure A-6 Model Diagram of WT4E1

Table A-7 Model Parameters of WT4E1 (Electrical Model)

Con No	Description	Value
1	Tfv - V-regulator filter	0.15
2	Kpv - V-regulator proportional gain	18
3	Kiv - V-regulator integrator gain	5
4	Kpp - T-regulator proportional gain	0.05
5	Kip - T-regulator integrator gain	0.1
6	Kf - Rate feedback gain	0
7	Tf - Rate feedback time constant	0.08
8	QMX - V-regulator max limit	0.47
9	QMN - V-regulator min limit	-0.47
10	IPMAX - Max active current limit	1.1
11	TRV - V-sensor	0
12	dPMX - Max limit in power PI controller (pu)	0.5
13	dPMN - Min limit in power PI controller (pu)	-0.5

Table A-7 -Continued

14	T_POWER - Power filter time constant	0.05
15	KQi - MVAR/Volt gain	0.1
16	VMINCL	0.9
17	VMAXCL	1.1
18	KVi - Volt/MVAR gain	120
19	Tv - Lag time constant in WindVar controller	0.05
20	Tp - Pelec filter in fast PF controller	0.05
21	ImaxTD - Converter current limit	1.7
22	Iphl - Hard active current limit	1.11
23	Iqhl - Hard reactive current limit	1.11

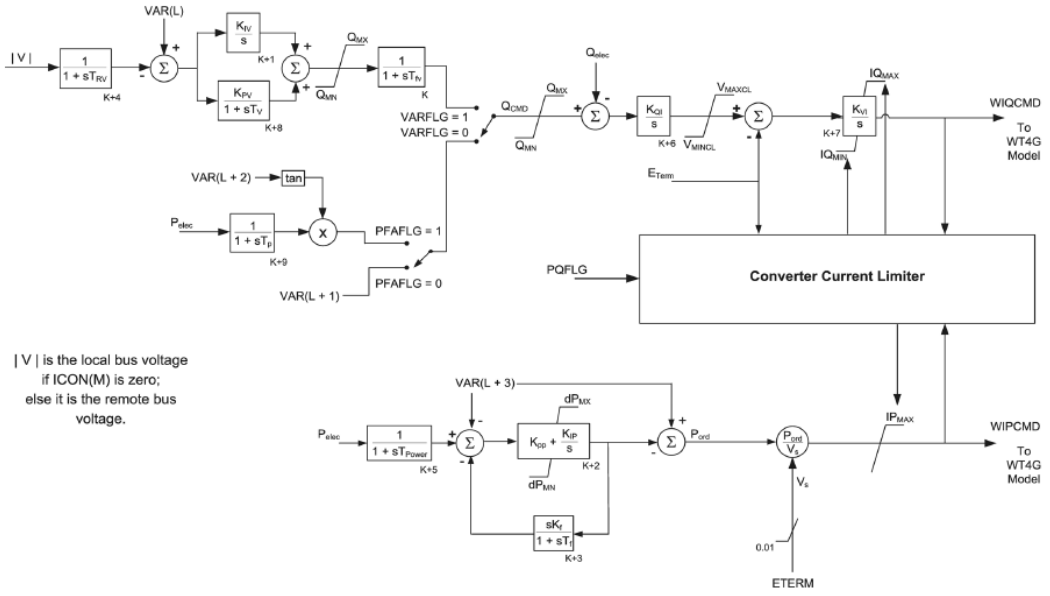

Figure A-7 Model Diagram of WT4E2

Table A-8 Model Parameters of WT4E2 (Electrical Model)

Con No	Description	Value
1	Tfv - V-regulator filter	0
2	Kpv - V-regulator proportional gain	15
3	Kiv - V-regulator integrator gain	2
4	Kpp - T-regulator proportional gain	0.08
5	Kip - T-regulator integrator gain	0.01
6	Kf - Rate feedback gain	0
7	Tf - Rate feedback time constant	0.08
8	QMX - V-regulator max limit	1
9	QMN - V-regulator min limit	-1.2
10	IPMAX - Max active current limit	1.1
11	TRV - V-sensor	0
12	dPMX - Max limit in power PI controller (pu)	0.5
13	dPMN - Min limit in power PI controller (pu)	-0.5
14	T_POWER - Power filter time constant	0.05
15	KQi - MVAR/Volt gain	0.01
16	VMINCL	0.875
17	VMAXCL	1.125
18	KVi - Volt/MVAR gain	55
19	Tv - Lag time constant in WindVar controller	0.05
20	Tp - Pelec filter in fast PF controller	0.05
21	ImaxTD - Converter current limit	1.115
22	Iphl - Hard active current limit	1.25
23	Iqhl - Hard reactive current limit	1.085
24	Tiqf - IQmax filter	0.02
25	FRT_Thres	0.875
26	FRT_Hys	0.05
27	FRT_Droop	0
28	FRT_Iq_Gain	2
29	Max_FRT_Iq	1
30	IQMax_Fact1	1
31	IQMax_Fact2	1
32	DC_Link_Droop	1
33	VinvMax0	1.1
34	Reactor Reactance	0.1415

References

[1] J. Brochu, C. Larose, and R. Gagnon, "Validation of Single- and Multiple-Machine Equivalents for Modeling Wind Power Plants," *Energy Conversion, IEEE Transactions on,* vol. 26, pp. 532-541, 2011.

[2] D. N. Kosterev, C. W. Taylor, and W. A. Mittelstadt, "Model validation for the August 10, 1996 WSCC system outage," *Power Systems, IEEE Transactions on,* vol. 14, pp. 967-979, 1999.

[3] "Final Report on the August 14, 2003 Blackout in the United States and Canada: Causes and Recommendations," *Issued by the U.S.-Canada Power System Outage Task Force, April 2004. [Online]. Available at: http://energy.gov/oe/downloads/blackout-2003-final-report-august-14-2003-blackout-united-states-and-canada-causes-and*.

[4] "Compliance Templates for the NERC Planning Standards," *North American Electric Reliability Council, June 1998. [Online]. Available at: http://www.nerc.com/comm/PC/Agendas%20Highlights%20and%20Minutes%20DL/1998/ct-9806a.pdf*.

[5] "Verification of Models and Data for Generator Excitation Control System or Plant Volt Var Control Functions," *NERC Standard MOD-026-1, December 10, 2012. [Online]. Available at: http://www.nerc.com/docs/standards/sar/MOD-026-1_clean_2012Dec11.pdf*.

[6] "Verification of Models and Data for Turbine Governor and Load Control or Active Power Frequency Control Functions," *NERC Standard MOD-027-1, October 4, 2012. [Online]. Available at: http://www.nerc.com/docs/standards/sar/MOD-027-1_clean_2012Sept11.pdf*.

[7] Q. Wei, R. G. Harley, and G. K. Venayagamoorthy, "Dynamic Modeling of Wind Farms with Fixed-Speed Wind Turbine Generators," in *Power Engineering Society General Meeting, 2007. IEEE*, 2007, pp. 1-8.

[8] A. Ellis, Y. Kazachkov, E. Muljadi, P. Pourbeik, and J. J. Sanchez-Gasca, "Description and technical specifications for generic WTG models — A status report," in *Power Systems Conference and Exposition (PSCE), 2011 IEEE/PES*, 2011, pp. 1-8.

[9] "WECC Guideline: WECC Wind Power Plant Dynamic Modeling Guide," *WECC Modeling and Validation Work Group, November 2010. [Online]. Available at http://renew-ne.org/wp-content/uploads/2012/05/WECCWindPlantDynamicModelingGuide.pdf*.

[10] "Global Wind Stats 2014 report," *GWEC,October, 2015. [Online]. Available at: http://www.gwec.net/wp-content/uploads/2015/02/GWEC_GlobalWindStats2014_FINAL_10.2.2015.pdf*.

[11] "U.S. Wind Industry Fourth Quarter 2014 Market Report," *American Wind Energy Association, Jan, 2015. [Online]. Available at: http://awea.files.cms-plus.com/4Q2014%20AWEA%20Market%20Report%20Public%20Version.pdf*.

[12] "ERCOT System Planning Report 2014," *ERCOT, Feb, 2014. [Online]. Available at: http://www.ercot.com/content/news/presentations/2014/System_Planning_Report_Feb%202014.pdf*.

[13] I. Erlich, J. Kretschmann, J. Fortmann, S. Mueller-Engelhardt, and H. Wrede, "Modeling of Wind Turbines Based on Doubly-Fed Induction Generators for Power System Stability Studies," *Power Systems, IEEE Transactions on,* vol. 22, pp. 909-919, 2007.

[14] K. Protsenko and X. Dewei, "Modeling and Control of Brushless Doubly-Fed Induction Generators in Wind Energy Applications," *Power Electronics, IEEE Transactions on,* vol. 23, pp. 1191-1197, 2008.
[15] R. Datta and V. T. Ranganathan, "Variable-speed wind power generation using doubly fed wound rotor induction machine-a comparison with alternative schemes," *Energy Conversion, IEEE Transactions on,* vol. 17, pp. 414-421, 2002.
[16] L. Mihet-Popa, F. Blaabjerg, and I. Boldea, "Wind turbine Generator modeling and Simulation where rotational speed is the controlled variable," *Industry Applications, IEEE Transactions on,* vol. 40, pp. 3-10, 2004.
[17] M. L. Ourari, L. A. Dessaint, and D. Van-Que, "Dynamic equivalent modeling of large power systems using structure preservation technique," *Power Systems, IEEE Transactions on,* vol. 21, pp. 1284-1295, 2006.
[18] "US Wind Industry Annual Market Report 2013," *AWEA, April 10, 2014. [Online]. Available at: http://www.awea.org/amr2013*
[19] "The Texas Renewable Energy Industry," *Texas Renewable Energy Industries Association, 2014. [Online]. Available at: https://texaswideopenforbusiness.com/sites/default/files/02/24/15/renewable_energy.pdf*
[20] P. Pourbeik, A. Ellis, J. Sanchez-Gasca, Y. Kazachkov, E. Muljadi, J. Senthil*, et al.*, "Generic stability models for type 3 & 4 wind turbine generators for WECC," in *Power and Energy Society General Meeting (PES), 2013 IEEE*, 2013, pp. 1-5.
[21] Y. Peng, T. Zhao, A. Wiesel, and A. Nehora, "Power System State Estimation Using PMUs With Imperfect Synchronization," *Power Systems, IEEE Transactions on,* vol. 28, pp. 4162-4172, 2013.
[22] H. Lina and L. Chen-Ching, "Parameter Identification With PMUs for Instability Detection in Power Systems With HVDC Integrated Offshore Wind Energy," *Power Systems, IEEE Transactions on,* vol. 29, pp. 775-784, 2014.
[23] F. Aminifar, M. Fotuhi-Firuzabad, A. Safdarian, A. Davoudi, and M. Shahidehpour, "Synchrophasor Measurement Technology in Power Systems: Panorama and State of the Art," *Access, IEEE,* vol. 2, pp. 1607-1628, 2014.
[24] A. G. Phadke, "Synchronized phasor measurements in power systems," *Computer Applications in Power, IEEE,* vol. 6, pp. 10-15, 1993.
[25] "Generic Models and Model Validation for Wind and Solar PV Generation: Technical Update," *Electric Power Research Institute, December 2011. [Online]. Available at: http://www.epri.com/abstracts/pages/productabstract.aspx?ProductID=000000000001021763&Mode=download*.
[26] "WECC Guideline: WECC Wind Power Plant Power Flow Modeling Guide," *WECC Modeling and Validation Work Group, November 2010. [Online]. Available at http://renew-ne.org/wp-content/uploads/2012/05/WECCWindPlantDynamicModelingGuide.pdf*.
[27] "PSSe MODEL LIBRARY," *Siemens Power Technologies International, Oct, 2013.*
[28] I. A. Hiskens and M. A. Pai, "Trajectory sensitivity analysis of hybrid systems," *Circuits and Systems I: Fundamental Theory and Applications, IEEE Transactions on,* vol. 47, pp. 204-220, 2000.
[29] Z. Huang, R. T. Guttromson, and J. F. Hauer, "Large-scale hybrid dynamic simulation employing field measurements," in *Power Engineering Society General Meeting, 2004. IEEE*, 2004, pp. 1570-1576 Vol.2.

[30] J. Ma, D. Han, W. J. Sheng, R. M. He, C. Y. Yue, and J. Zhang, "Wide area measurements-based model validation and its application," *Generation, Transmission & Distribution, IET,* vol. 2, pp. 906-916, 2008.
[31] I. A. Hiskens and M. A. Pai, "Power system applications of trajectory sensitivities," in *Power Engineering Society Winter Meeting, 2002. IEEE*, 2002, pp. 1200-1205 vol.2.
[32] I. A. Hiskens, "Power system modeling for inverse problems," *Circuits and Systems I: Regular Papers, IEEE Transactions on,* vol. 51, pp. 539-551, 2004.
[33] I. A. Hiskens and J. Alseddiqui, "Sensitivity, Approximation, and Uncertainty in Power System Dynamic Simulation," *Power Systems, IEEE Transactions on,* vol. 21, pp. 1808-1820, 2006.
[34] A. Ketabi, S. M. Nosratabadi, and M. R. Sheibani, "Optimal PMU placement based on Mean Square Error using Differential Evolution algorithm," in *Power Quality Conference (PQC), 2010 First*, 2010, pp. 1-6.
[35] Y. del Valle, G. K. Venayagamoorthy, S. Mohagheghi, J. C. Hernandez, and R. G. Harley, "Particle Swarm Optimization: Basic Concepts, Variants and Applications in Power Systems," *Evolutionary Computation, IEEE Transactions on,* vol. 12, pp. 171-195, 2008.
[36] F. Benhamida, Y. Salhi, S. Souag, A. Graa, Y. Ramdani, and A. Bendaoud, "A PSO algorithm for economic scheduling of power system incorporating wind based generation," in *Modeling, Simulation and Applied Optimization (ICMSAO), 2013 5th International Conference on*, 2013, pp. 1-6.
[37] S. Li, D. Zhao, X. Zhang, and C. Wang, "Reactive power optimization based on an improved quantum discrete PSO algorithm," in *Critical Infrastructure (CRIS), 2010 5th International Conference on*, 2010, pp. 1-5.
[38] T. Hawkins, W. N. White, H. Guoqiang, and F. D. Sahneh, "Region II wind power capture maximization using robust control and estimation with alternating gradient search," in *American Control Conference (ACC), 2011*, 2011, pp. 2695-2700.
[39] L. Dung Anh and V. Dieu Ngoc, "Optimal reactive power dispatch by pseudo-gradient guided particle swarm optimization," in *IPEC, 2012 Conference on Power & Energy*, 2012, pp. 7-12.
[40] W. Siever, R. P. Kalyani, M. L. Crow, and D. R. Tauritz, "UPFC control employing gradient descent search," in *Power Symposium, 2005. Proceedings of the 37th Annual North American*, 2005, pp. 379-382.
[41] M. A. M. Ariff, B. C. Pal, and A. K. Singh, "Estimating Dynamic Model Parameters for Adaptive Protection and Control in Power System," *Power Systems, IEEE Transactions on,* vol. 30, pp. 829-839, 2015.
[42] M. Botao, R. Zane, and D. Maksimovic, "System identification of power converters with digital control through cross-correlation methods," *Power Electronics, IEEE Transactions on,* vol. 20, pp. 1093-1099, 2005.
[43] Y. Gao and R. Billinton, "Adequacy assessment of generating systems containing wind power considering wind speed correlation," *Renewable Power Generation, IET,* vol. 3, pp. 217-226, 2009.
[44] R. Jalayer and B. T. Ooi, "Co-Ordinated PSS Tuning of Large Power Systems by Combining Transfer Function-Eigenfunction Analysis (TFEA), Optimization, and Eigenvalue Sensitivity," *Power Systems, IEEE Transactions on,* vol. 29, pp. 2672-2680, 2014.

[45] R. J. Koessler, F. S. Prabhakara, and A. H. Al-Mubarak, "Analysis of Oscillations with Eigenanalysis and Prony Techniques," in *Power Engineering Society General Meeting, 2007. IEEE*, 2007, pp. 1-8.

[46] S. Y. Sun, H. C. Shu, J. Dong, and Z. J. Liu, "Analysis of low frequency oscillation mode based on PMU and PRONY method," in *Electric Power Conference, 2008. EPEC 2008. IEEE Canada*, 2008, pp. 1-4.

Biographical Information

Xueyang Cheng received the Bachelor's degree in Electrical Engineering from the Shandong University, China, in 2010.

In August 2010, he started PhD porgram in the area of power system dynamic stability analysis and power system model parameter identification at the University of Texas at Arlington (UTA). He is also a member of the research group at the Energy Systems Research Center at UTA. His areas of interest are power system dynamic stability analysis and control, power system operations and wind farm modeling.